


EXHIBIT D

PATENT
28967/34891

IN THE UNITED STATES PATENT AND TRADEMARK OFFICE

Applicant(s): Alitalo et al.)	I hereby certify that this paper is being
)	deposited with the United States Postal
Serial No: 09/169,079)	Service with sufficient postage as first class
)	mail in an envelope addressed to:
Filed: October 9, 1998)	Commissioner for Patents, Washington,
)	D.C., 20231 on this date:
Title: Flt4 (VEGFR-3) as a Target for)	
Tumor Imaging and Anti-Tumor Therapy)	Date: <u>JANUARY 31</u> , 2001
)	
)	
Group Art Unit: 1646)	
)	David A. Gass
Examiner: J. Murphy)	Registration No. 38,153
)	Attorney for Applicants

Declaration Pursuant to 37 C.F.R. § 1.132 of Kari Alitalo

I, Dr. Kari Alitalo, declare and state as follows:

Introduction

I am a co-inventor of subject matter of the above-identified patent application (hereinafter "the patent application"). I make this declaration to provide evidence to the Patent Office that may be relevant to the patentability of pending claims in the patent application that relate to methods of treatment. Specifically, I understand from my attorneys that the Patent Office has reviewed the patent application and has alleged that the application does not adequately teach how to effectively treat any disease or reach any therapeutic endpoint in humans by administering a composition comprising a compound to inhibit Flt4 binding to its ligand(s). This declaration is intended to provide evidence of therapeutic efficacy for the methods described and claimed in the patent application.

Evidence

Since the patent application was filed, my laboratory and others have obtained additional research results that evince the therapeutic efficacy of the methods of treatment described and claimed in the patent application. I summarize the protocols and data below.

I. EXAMPLE 1: SOLUBLE FLT4 INHIBITS VEGF-C-MEDIATED TUMOR GROWTH AND METASTASIS

A. OVERVIEW

MCF-7 human breast carcinoma cells overexpressing recombinant VEGF (VEGF-A) or VEGF-C were orthotopically implanted into SCID mice. The VEGF-C overexpression increased tumor growth but, unlike VEGF-A overexpression, it had little effect on tumor angiogenesis. On the other hand, VEGF-C strongly promoted the growth of tumor associated lymphatic vessels, which in the tumor periphery were commonly infiltrated with the tumor cells. *These effects of VEGF-C were inhibited by a soluble VEGFR-3 fusion protein.* These data indicate that VEGF-C can upregulate tumor growth and/or metastasis via the lymphatic vessels, presumably through the Flt4 (VEGFR-3) receptor which is expressed in lymphatic vessels, and that the tumor growth/metastasis can be inhibited by blocking the interaction between VEGF-C and Flt4. In particular, a polypeptide comprising a soluble Flt4 extracellular domain fragment that binds VEGF-C can be used to inhibit this tumor growth/metastasis.

B. MATERIALS AND METHODS

1. Preparation of plasmid expression vectors

The cDNAs coding for the human VEGF-C or VEGF₁₆₅ were introduced into the pEBS7 plasmid (Peterson and Legerski, *Gene*, 107: 279-84 (1991)). The same vector was used for the expression of the soluble receptor chimeras VEGFR-3-Ig, containing the first three immunoglobulin homology domains of VEGFR-3 fused to the Fc-domain of human immunoglobulin γ chain and VEGFR-1-Ig, containing the first five Ig homology domains of VEGFR-1 in a similar construct (Achen, *et al.*, *Proc Natl Acad Sci U S A*, 95: 548-53 (1998)). These plasmids were used to transfect cancer cell lines as described below.

2. Production and analysis of transfected cells

The MCF-7S1 subclone of the human MCF-7 breast carcinoma cell line was transfected with the plasmid DNA by electroporation and stable cell pools were selected and cultured as previously described (Egeblad and Jaattela, *Int J Cancer*, 86: 617-25, 2000).

The following procedures were used to confirm transgene expression in transfected cells. The cells transformed with VEGF or VEGF-C transgenes were metabolically labeled in methionine and cysteine free MEM (Gibco) supplemented with 100 μ Ci/ml [35 S]-methionine and [35 S]-cysteine (Redivue Pro-Mix, Amersham Pharmacia Biotech). The labeled growth factors were immunoprecipitated from the conditioned medium using antibodies against VEGF-C (Joukov, *et al.*, *EMBO J*, 16: 3898-911 (1997)) or VEGF (MAB293, R & D Systems). The immunocomplexes and the VEGFR-Ig fusion proteins were precipitated using protein A sepharose (Amersham Pharmacia Biotech), washed twice in 0.5% BSA, 0.02% Tween 20 in PBS and once in PBS and analyzed in SDS-PAGE under reducing conditions.

3. Cell proliferation and tumorigenesis assays

Cells (20 000/well) were plated in quadruplicate in 24-wells, trypsinized on replicate plates after 1, 4, 6, or 8 days and counted using a hemocytometer. Fresh medium was provided after 4 and 6 days. For the tumorigenesis assay, sub-confluent cultures were harvested by trypsination and washed twice, and 10^7 cells in PBS were inoculated into the fat pads of the second (axillar) mammary gland of ovariectomized SCID mice, carrying subcutaneous 60-day slow-release pellets containing 0.72 mg 17β -estradiol (Innovative Research of America). The ovariectomy and implantation of the pellets were performed 4-8 days before tumor cell inoculation. Tumor length and width were measured twice weekly in a blinded manner, and the tumor volume was calculated as the length x width x depth x 0.5, assuming that the tumor is a hemi-ellipsoid and the depth is the same as the width (Benz *et al.*, *Breast Cancer Res. Treat.*, 24: 85-95 (1993)).

4. Histology and quantitation of the blood vessels

The tumors were excised, fixed in 4% paraformaldehyde (pH 7.0) for 24 hours, and embedded in paraffin. Sections (7 μ m) were immunostained with monoclonal

antibodies against PECAM-1 (Pharmingen), VEGFR-3 (Kubo *et al.*, *Blood*, 96: 546-553 (2000)) or PCNA (Zymed Laboratories) or polyclonal antibodies against LYVE-1 (Banerji *et al.*, *J Cell Biol*, 144: 789-801 (1999)), VEGF-C (Joukov *et al.*, *EMBO J*, 16: 3898-911 (1997)) or laminin according to published protocols (Partanen *et al.*, *Cancer*, 86: 2406-12 (1999)). The average of the number of the PECAM-1 positive vessels was determined from three areas (60x magnification) of the highest vascular density (vascular hot spots) in a section. All histological analysis was performed using blinded tumor samples.

5. Adenoviral expression of soluble VEGFR-3 and Evan's blue draining assay

The cDNA coding for the VEGFR-3-Ig fusion protein was subcloned into the pAdBglII plasmid and the adenoviruses produced as previously described (Laitinen *et al.*, *Hum Gene Ther.*, 9: 1481-6 (1998)). The VEGFR-3-Ig or LacZ control (Laitinen *et al.*, *Hum Gene Ther.*, 9: 1481-6 (1998)) adenoviruses, 10⁹ pfu/mouse, were injected intravenously into the SCID mice 3 hours before the tumor cell inoculation. After 3 weeks, four mice from each group were narcotized, the ventral skin was opened, and a few microliters 3% Evan's blue dye (Sigma) in PBS were injected into the tumor. The drainage of the dye from the tumor was followed macroscopically.

C. RESULTS

1. VEGF-C and VEGFR-3-Ig Expression do not affect MCF-7 cell growth *in vitro*.

The MCF-7 human breast carcinoma cells were transfected with expression plasmids coding for full length human VEGF-C or a soluble VEGFR-3 fusion protein (VEGFR-3-Ig) as described above, and stable cell pools were selected. For comparison, human VEGF₁₆₅ or VEGFR-1-Ig were expressed in the same cells. Immunoprecipitation was used to analyze the conditioned media of these cells for the efficient production and secretion of the proteins. Immunoprecipitates of VEGF-C, VEGF or the soluble receptor proteins from metabolically labeled MCF-7 cells were analyzed in PAGE under reducing conditions.

This investigation revealed that overexpression of VEGF-C, VEGF, soluble VEGFR-3 fusion protein, or soluble VEGFR-1 fusion protein does not affect the proliferation

of the MCF-7 breast carcinoma cells *in vitro*. When the cells were seeded in 24-well plates and their growth was measured using hemacytometer, it was found that the growth rate of the transfected cells was not affected.

2. VEGF-C increases tumor growth without affecting tumor angiogenesis

To determine the *in vivo* effects of VEGF-C, the MCF-7 cell pools were implanted into the mammary fat pads of ovariectomized SCID mice carrying slow-release estrogen pellets to provide a constant level of the hormone needed to support the growth of the MCF-7 tumors.

Overexpression of VEGF-C increased tumor growth significantly (VEGF-C: $545 \text{ mm}^3 \pm 110 \text{ mm}^3$, control: $268 \text{ mm}^3 \pm 69 \text{ mm}^3$ at 13 days, $n=8$, $p<0.0001$, Student's t-test). The effect of VEGF-C overexpression on tumor growth was much less dramatic than that of VEGF-A (VEGF-A: $1136 \text{ mm}^3 \pm 339 \text{ mm}^3$, control: $189 \text{ mm}^3 \pm 57 \text{ mm}^3$, at 15 days, $n=6$, $p<0.0001$, Student's t-test). The increased tumor growth was neutralized by mixing the VEGF-C or VEGF overexpressing MCF-7 cells with cells expressing the soluble VEGFR-3 or VEGFR-1 fusion proteins, respectively. Further, it was found that the increased growth of the VEGF-C overexpressing tumors also was inhibited by a circulating soluble VEGFR-3-Ig expressed in the liver by an intravenously injected recombinant adenovirus.

To investigate the effect of VEGF-C on tumor angiogenesis, sections of the tumors were stained for PECAM-1, an endothelial antigen primarily expressed in blood vessels and only weakly in lymphatic vessels. Quantitation of the PECAM-1 positive vessels in the tumors revealed that overexpression of VEGF-C had very little effect on the density of the tumor blood vessels (40.2 ± 12.2 vessels/microscopic field for VEGF-C tumors, $n=18$ and 36.6 ± 11.6 for control tumors, $n=23$, average of three different experiments). In contrast, overexpression of VEGF-A increased the vascular density approximately two-fold.

3. VEGF-C overexpression is associated with lymphangiogenesis and intralymphatic growth of tumor cells

The effect of VEGF-C on tumor associated lymphatic vessels was analysed by immunostaining for the lymphatic specific marker LYVE-1 (Banerji *et al.*, *J Cell Biol*, 144: 789-801 (1999)). This marker revealed highly hyperplastic lymphatic vessels in the periphery

of the VEGF-C overexpressing tumors. The proliferating cell nuclear antigen (PCNA) was detected in many of the LYVE-1 positive endothelial cells, showing that these lymphatic vessels were actively proliferating. Confirmation of the lymphatic identity of the vessels was obtained by staining for VEGFR-3 and by the lack of staining for the basal lamina component laminin. Thin lymphatic vessels were also present inside some of the VEGF-C overexpressing tumors.

The lymphatic vessels in the tumor periphery were commonly infiltrated by the VEGF-C positive tumor cells. In a striking contrast, the VEGF-overexpressing and control tumors contained no or only few lymphatic vessels.

4. VEGF-C-induced lymphangiogenesis is inhibited by a circulating soluble VEGFR-3 fusion protein

In human breast cancer, the centinel node method is used to trace lymphatic drainage and metastatic spread (for a review, see Parker *et al.*, *Radiol Clin North Am*, 38: 809-23 (2000)). In order to trace lymphatic drainage of the MCF-7 tumors, Evan's blue dye was injected into VEGF-C-overexpressing or control tumors in mice infected with VEGFR-3-Ig or control adenovirus. Control experiments indicated that infection of cultured human embryonic kidney cells with the VEGFR-3-Ig adenovirus resulted in the secretion of high amounts of the soluble VEGFR-3-Ig fusion protein and intravenous infection of mice led to high systemic levels of the VEGFR-3-Ig fusion protein in the serum. Injection of Evan's blue dye into the tumors resulted in the staining of lymphatic but not blood vessels and revealed an increased number of enlarged lymphatic vessels surrounding the VEGF-C overexpressing tumors when compared to control tumors. Most of the enlarged lymphatic vessels were absent from VEGF-C overexpressing tumors in mice treated with the VEGFR-3-Ig adenovirus.

D. ANALYSIS

The foregoing data demonstrate that VEGF-C overexpression in MCF-7 mammary tumors strongly and specifically induces the growth of tumor associated lymphatic vessels, but does not have major effects on tumor angiogenesis. Furthermore, it demonstrated that **VEGF-C-mediated increased tumor growth and tumor-associated**

lymphangiogenesis were inhibited by a soluble VEGFR-3 fusion protein, *i.e.*, an agent selected to block VEGF-C-mediated stimulation of endothelial cells that express VEGFR-3.

Here, it is shown that overexpression of VEGF-C can induce the growth of lymphatic vessels in association with experimental tumors. The VEGF-C induced lymphatic vessels in the tumor periphery were highly hyperplastic and mostly filled with tumor cells, whereas the lymphatic vessels inside the tumor were flattened and without a lumen. Unlike lymphatic endothelial cells in normal adult tissues, the lymphatic endothelial cells associated with the MCF-7 tumors were actively proliferating. Thus, it would appear that most of the peri- and intratumoral lymphatic vessels were generated by proliferation of the endothelial cells of pre-existing lymphatic vessels.

The spread of cancer through the lymphatics into the regional lymph nodes has long been an important prognostic indicator in clinical use. The growth of tumor cells inside the enlarged lymphatic vessels associated with the VEGF-C-overexpressing tumors as demonstrated in this Example, closely resembles the peritumoral lymphatic invasion, that correlates with metastatic spread to the lymph nodes and poor survival in human breast cancer (Lauria *et al.*, *Cancer*, 76: 1772-8 (1995)). Thus, the data reported herein provides evidence that expression of VEGF-C promotes tumor metastasis via the lymphatic system.

The effect of VEGF-C on tumor growth was not simply due to variation between the cell pools, as shown by the ability of the VEGFR-3 fusion protein to inhibit the growth of VEGF-C overexpressing tumors. By injecting Evan's blue dye into the tumors, it was demonstrated that an increased number of large draining lymphatic vessels were associated with the VEGF-C-overexpressing tumors. It is possible that the higher number of functional lymphatic vessels may result in a better lymphatic drainage and thus a lower interstitial pressure and enhanced blood perfusion of the VEGF-C-overexpressing tumors. Irrespective of whether VEGF-C/D - VEGFR-3 mediated tumor progression for a particular tumor proceeds through angiogenesis, lymphangiogenesis, or both, the therapeutic methods described and claimed in the patent application should inhibit these processes, by blocking VEGF-C or -D mediated stimulation of VEGFR-3.

In conclusion, the results above show that VEGF-C produced by tumor cells can induce the growth of lymphatic vessels around tumors and thus facilitate the growth and

intralymphatic spread of cancer. The data further indicates that inhibition of tumor-associated lymphangiogenesis, for example using soluble VEGFR-3 proteins as therapeutics, represents a valuable and effective way of inhibiting tumor metastasis *in vivo*.

II. EXAMPLE 2: INHIBITION OF TUMOR ANGIOGENESIS *IN VIVO* WITH AN ANTI-FLT4 MONOCLONAL ANTIBODY

Attached hereto as Exhibit A is a copy of the recently published journal article Kubo et al., "Involvement of vascular endothelial growth factor receptor-3 in maintenance of integrity of endothelial cell lining during tumor angiogenesis," *Blood*, 96(2): 546-553 (15 July 2000). I am a co-author of the paper and confirm that the experiments and results reported therein are correct, and I incorporate that paper ("the *Blood* paper") into this declaration by reference.

As reported in the *Blood* paper, we generated a monoclonal antibody specific to Flt4 (VEGFR-3) and confirmed that the antibody (designated AFL4) was specific for Flt4 and was capable of blocking VEGF-C binding and stimulation of Flt4. In healthy adult mice, the antibody stained only lymphatic tissue, indicating that Flt4 expression is largely restricted to lymphatic endothelia in adults. These results are consistent with other studies of healthy adult tissues.

To examine the role of Flt4 and anti-Flt4 therapy in cancers, tumor cells (rat C6 glioblastoma or human PC-3 prostate adenocarcinoma) were transplanted subcutaneously in mice. Both cell lines have been shown to secrete VEGF-C, and the C6 glioblastoma has been shown to secrete VEGF, an angiogenic growth factor that binds VEGFR-1 and -2, but not Flt4/VEGFR-3. The anti-Flt4 monoclonal antibody AFL4 was injected on alternating days for twelve days into the mice in controlled studies. As shown in Figure 4A and Table 1 and reported at page 549 of the *Blood* paper, the AFL4 antibody inhibited growth of the aggressive C6 tumor, and prevented any detectable growth of the slower growing PC-3 tumor.

Histological examination of the glioblastoma tumor-bearing mice revealed that Flt4/VEGFR-3 was being expressed in endothelia of intratumoral blood vessels. (See p. 550.) Interestingly, the vascular trunk governing tumor blood supply was smaller in the antibody-treated mice than in the controls. Many micro-hemorrhages were found in vessels

of the antibody-treated mice, suggesting that the anti-Flt4 antibody was interfering with the integrity of the endothelial sheet during neo-angiogenesis.

These data provide further *in vivo* evidence implicating Flt4 receptor in tumor neo-angiogenesis, even though the receptor's expression become largely restricted to lymphatic endothelia in healthy adult tissue. Moreover, the data provide evidence that agents that target and disrupt the interaction between Flt4 and its ligands, thereby inhibiting Flt4 signaling, have indications for inhibiting cancer growth.

III. EXAMPLE 3: INHIBITION OF LYMPHANGIOGENESIS IN MICE EXPRESSING SOLUBLE VEGFR-3/FLT4

A. OVERVIEW

The previous two Examples indicated that VEGF-C and Flt4 are involved in *in vivo* tumor growth, apparently through mechanisms involving lymphatic vessels in some tumors, blood vessels in other tumors (and of course, possibly both types of vessels in some tumors). These effects of VEGF-C were inhibited *in vivo* by a soluble Flt4 fusion protein in Example I, and anti-Flt4 antibody in Example II. The present Example provides further evidence that soluble VEGFR-3 is a potent inhibitor of VEGF-C/VEGF-D signaling *in vivo* and, when expressed in the skin of transgenic mice, it inhibits lymphangiogenesis and induces a regression of already formed lymphatic vessels while the blood vasculature remains intact. Thus, the data in this example shows that therapy designed to block Flt4 interaction with its ligands can be effective for modulating the growth of tissues such as lymphatic vessels that express Flt4.

More particularly, the present example shows that a chimeric protein consisting of the ligand-binding portion of the extracellular portion of VEGFR-3, joined to the Fc domain of immunoglobulin (Ig) γ -chain (VEGFR-3-Ig) neutralizes the activity of VEGF-C and VEGF-D and inhibits the formation of the dermal lymphatic vasculature when expressed in mouse epidermis under the keratin-14 (K14) promoter. As the blood vessel network remained normal in these mice, the inhibition appears to be specific to the lymphatic vessels that express Flt4. Of course, an inhibitory effect on tumor angiogenesis would still be expected in the case of tumor neovascularization that is characterized and mediated by Flt4 expression and activity, as in Example II.

B. MATERIALS AND METHODS

1. Production of VEGF-C, VEGF-D and VEGFR-Ig Fusion Proteins

The mature form of human VEGF-C was produced as described above and by Joukov *et al.*, (*EMBO J.* 16: 3898-3911 (1997)). VEGF-D was obtained from R&D Systems (Minneapolis, Minnesota). The VEGFR-1-Ig and VEGFR-3-Ig proteins consisting of the ligand-binding domains of human VEGFRs fused to human IgG1 Fc domain were produced in *Drosophila* S2 cells (Invitrogen, Carlsbad, California).

2. VEGFR-3 bioassay

Ba/F3 cells expressing a VEGFR-3/EpoR chimera comprising the VEGFR-3 extracellular domain fused to the intracellular domain of an erythropoietin receptor (Achen, *Eur. J. Biochem.*, 267: 2505–2515 (2000)) were seeded, in 96-well microtiter plates at 15,000 cells/well in triplicates supplied with 100 ng/ml of VEGF-C and with indicated concentrations of VEGFR-Ig proteins. After 48 hours, the viability of the cells was determined by adding MTT (3-(4,5-dimethylthiazol-2-yl)-2,5-diphenyl tetrazolium bromide (Sigma), 0.5 mg/ml), followed by further 2 hours of culture, addition of an equal volume of cell lysis solution (10% SDS, 10 mM HCl) and incubation overnight at 37 °C. Absorbance was measured at 540 nm.

3. Generation of the transgenic mice

The sequence encoding human VEGFR-3 Ig-homology domains 1–3 was amplified using PCR. The primers employed for this purpose were:

5'-TACAAAGCTTTTCGCCACCATGCAG-3' and

5'-TACAGGATCCTCATGCACAATGACCTC-3'.

The PCR product was cloned into the plg-plus vector (Ingenius, R&D Systems) in frame with human IgG1 Fc tail. The VEGFR-3-Ig construct was then transferred into the human keratin-14 promoter-expression vector. The expression cassette fragment was injected into fertilized mouse oocytes of the FVB/NIH and DBAxBalbC hybrid strains to create seven lines of K14-VEGFR-3-Ig mice. Transgene expression was analyzed and the phenotype was confirmed from all three founder lines expressing the transgene as described below.

4. Analysis of transgene expression

For northern blotting, 10 µg of total RNA extracted from skin in 1 % agarose was subjected to electrophoresis, transferred to nylon filters (Nytran), hybridized with the corresponding [³²P]-labeled cDNA probes and exposed autoradiography. For western blotting, skin biopsies were homogenized into the lysis buffer (20 mM Tris, pH 7.6, 1 mM EDTA, 50 mM NaCl, 50 mM NaF, 1% Triton-X100) supplemented with 1 mM PMSF, 1 mU/ml aprotinin, 1 mM Na₃VO₄ and 10 µg/ml leupeptin. The Ig-fusion proteins were precipitated from 1 mg of total protein and separated in SDS-PAGE, transferred to nitrocellulose and detected using the horseradish peroxidase conjugated rabbit antibodies against human IgG (DAKO, Carpinteria, California) and the enhanced chemiluminescence detection system.

5. Immunohistochemistry and TUNEL staining

Paraffin sections (5 µm) from 4% paraformaldehyde (PFA) fixed tissues were stained using rat monoclonal antibodies against mouse VEGFR-3 (Kubo *et al.*, *Blood* 96:546-553, 2000) or CD31/PECAM-1 (PharMingen, San Diego, California), rabbit polyclonal antibodies against mouse LYVE-1 (Banerji *et al.*, *J Cell Biol*, 144: 789-801, 1999), or biotinylated mouse monoclonal antibodies against human IgG Fc domain (Zymed, San Diego, California). For TUNEL staining, detection of DNA fragmentation was done using *in situ* Cell Death Detection Kit (fluorescein; Roche, Indianapolis, IN).

6. Visualization of blood and lymphatic vessels

For visualization of blood vessels (Thurston *et al.*, *Science* 286: 2511–2514 (1999)), 100 µl of 1 mg/ml biotinylated *Lycopersicon esculentum* lectin (Sigma) was injected (IV) by the femoral vein and allowed to circulate for 2 minutes. After fixation by perfusion with 1% PFA/0.5% glutaraldehyde in PBS, bound lectin was visualized by the ABC-3,3'-diaminobenzidine peroxidase reaction. In VEGFR-3 +/-LacZ mice, the lymphatic vessels were then stained by the β-galactosidase substrate X-Gal (Sigma, St. Louis, MO). For the visualization of functional lymphatic vessels, Evans blue dye (5 mg/ml; Sigma, St. Louis, MO) was injected into the footpad of the hindlimb or TRITC-dextran (Sigma, 8 mg/ml) was

injected into the ear or tail and the lymphatic vessels were analysed by light or fluorescence microscopy, respectively.

7. Detection of the VEGFR-3-Ig protein in serum

ELISA plates (Nunc Maxisorp, Copenhagen, Denmark) were coated with mouse antibodies against human IgG (Zymed, 2 µg/ml in PBS) or human VEGFR-3 (clone 7B8, 4 µg/ml). The mouse sera were diluted into the incubation buffer (5 mg/ml BSA, 0.05 % Tween 20 in PBS) and allowed to bind for 2 hours at room temperature. The plates were then washed 3 times with incubation buffer before addition of mouse anti-human IgG1 (Zymed, 1:500) for 1 hour. Streptavidin conjugated with alkaline phosphatase (Zymed, 1:5000) was then incubated in the wells for 30 minutes, followed by addition of the substrate (1 mg/ml p-Nitrophenyl phosphate in 0.1 M diethanolamine, pH 10.3) and absorbance reading at 405 nm.

8. Magnetic resonance imaging

MRI data was acquired using a s.m.i.s. console (Surrey Medical Imaging Systems, Guildford, UK) interfaced to a 9.4 T vertical magnet (Oxford Instruments, Oxford, UK). A single loop surface coil (diameter 35 mm) was used for signal transmission and detection. A T₂-weighted (TR 2000 ms, TE 40 ms, 4 scans/line) multislice spin-echo sequence was used with an FOV of 25.6 mm² (matrix size: 256 × 128) and slice thickness of 1.3 mm in transverse orientation. Saturation pulses centered at 1.2 ppm were used to decrease fat signals in T₂-images. Diffusion weighted MRI was acquired using monopolar diffusion gradients (b-value ≈ 800 s/mm²) along slice axis in the spin-echo sequence (TR 2000 ms, TE 40 ms), and water apparent diffusion coefficient (ADC) was computed by fitting the MRI data as function of b-values into a single exponential.

C. RESULTS

1. Soluble VEGFR-3 inhibits VEGF-C-mediated signaling *in vitro*

To inhibit VEGF-C signaling through VEGFR-3, a fusion protein consisting of the first three Ig-homology domains of VEGFR-3 and IgG Fc domain was employed. The VEGFR-3-Ig bound VEGF-C and VEGF-D with the same efficiency as the full-length

extracellular domain and inhibited VEGF-C–induced VEGFR-3 phosphorylation and subsequent p42/p44 mitogen-activated protein kinase (MAPK) activation in VEGFR-3 expressing endothelial cells. In contrast, a similar VEGFR-1– Ig fusion protein, which does not bind VEGF-C, did not affect p42/p44 MAPK activation.

The effect of soluble VEGFR-3 on VEGF-C signaling also was determined in a bioassay using a chimeric VEGFR-3/erythropoietin (Epo) receptor capable of transmitting VEGF-C dependent survival and proliferation signals for the IL-3 dependent Ba/F3 cells in the absence of IL-3 (Achen et al., Eur. J. Biochem., 267:2505-2515, 2000). In this cellular assay, there was a complete inhibition of VEGF-C–dependent cell survival at a 0.5:1 molar ratio (VEGFR-3–Ig:VEGF-C), whereas VEGFR-1-Ig had no effect. Similarly, VEGFR-3–Ig also abolished VEGF-D–induced survival of the VEGFR-3/EpoR cells. In contrast, even a ten-fold molar excess of VEGFR-2–Ig only partially abolished VEGF-C dependent viability, perhaps because of lower affinity of VEGF-C to VEGFR-2.

2. Soluble VEGFR-3 inhibits the formation of lymphatic vessels *in vivo*

To determine the inhibitory effect of VEGFR-3–Ig *in vivo*, the fusion protein was expressed under the control of K14 promoter, which directs transgene expression to the basal epidermal cells of the skin. VEGFR-3–Ig expression was detected in mice by northern blotting of skin RNA and by western blotting of protein extracts from the skin. These mice appeared healthy and fertile and had a normal lifespan. Histological examination of the skin revealed a thickened dermis and subcutaneous layer. Antibody staining confirmed VEGFR-3–Ig expression in the basal keratinocytes. When the skin sections were stained for markers of the lymphatic endothelium, VEGFR-3 (Jussila *et al.*, *Cancer Res.*, 58: 1599-1604 (1998); Kubo *et al.*, *Blood*, 96: 546-553 (2000)) and LYVE-1 (Banerji *et al.*, *J. Cell Biol.*, 144: 789-801 (1999)), no lymphatic vessels were observed in the transgenic mice, even though lymphatic vessels were stained in the skin of control mice. In contrast, blood vessels were stained for the panendothelial marker PECAM-1/CD31 in both transgenic and wild-type skin.

3. Soluble VEGFR-3 suppresses lymphangiogenesis but not angiogenesis

In order to visualize better the lymphatic vessels, the K14- VEGFR-3-Ig mice were mated with heterozygous VEGFR-3+/LacZ mice that express β -gal in the *Flt4* locus (Dumont *et al.*, *Science* 282: 946–949, (1998)). When whole-mount tissue preparations of the ear skin were stained using the substrate X-gal, no lymphatic vessels were detected, whereas, in the control mice, blue-staining lymphatic vessels were visualized. In vascular perfusion staining using biotin-labeled lectin (Thurston *et al.*, *Science* 286: 2511–2514 (1999)), the blood vessels appeared normal in the K14-VEGFR-3-Ig mice.

The absence of the lymphatic vessels also was confirmed using a functional assay, monitoring the fate of Evans blue dye or TRITC-dextran injected into the skin. The dye was rapidly collected into the lymphatic vessels surrounding the ischiatic vein after injection into the hindlimb footpads of wild-type mice, whereas no dye was seen in such vessels in the transgenic mice where collecting lymphatic vessels were either absent or rudimentary. The lymphatic vessels in control mice also were visualized using fluorescence microscopy for TRITC-dextran injected intradermally into the ear or tail, whereas no such vessels were seen in the transgenic mice.

4. Circulating soluble VEGFR-3 is associated with a transient loss of lymphatic tissue in internal organs

By the age of two weeks, the VEGFR-3-Ig/VEGFR-3+/LacZ mice had only a few thin and rudimentary, if any, lymphatic vessels in organs such as diaphragm, heart, lungs, caecum, pancreas, mesenterium and esophagus when compared with the control VEGFR-3+/LacZ littermate mice. Such findings, obtained by X-Gal staining, were confirmed by immunostaining for VEGFR-3 and LYVE-1. In addition, the lack of lymphatic vessels in heart pericardium was associated with pericardial fluid accumulation in at least some of the mice. At three weeks of age, regrowth of the lymphatic vessels was apparent. In adult transgenic mice, only some organs such as heart and diaphragm had abnormally patterned and incompletely developed lymphatic vessels.

The effects seen in the internal organs indicate that the soluble VEGFR-3-Ig protein circulates in the bloodstream. Indeed the fusion protein was detected in the serum of the transgenic mice using a specific enzyme-linked immunosorbent assay; the levels ranged

between 100–200 ng/ml, being highest in the young mice. Based on our *in vitro* experiments, such concentrations would neutralize about 20–40 ng/ml of VEGF-C. The VEGFR-3-Ig protein was relatively stable in the bloodstream, as intravenously injected recombinant VEGFR-3-Ig was in the serum for at least nine hours.

5. The transgenic phenotype has features of human lymphedema

The K14-VEGFR-3-Ig mice were distinguished from their wild-type littermates by the swelling of their feet, which was already visible at birth. Older mice showed thickening of the skin, dermal fibrosis and increased deposition of subcutaneous fat. Magnetic resonance imaging (MRI) revealed prominent T₂-hyperintense regions in foot skin and subcutaneous tissues of the transgenic mice indicating increased fluid accumulation, whereas similar regions were absent in littermate controls. The apparent diffusion coefficient (ADC) for these hyperintense areas was $1.99 [0.60] \times 10^{-3} \text{ mm}^2/\text{s}$, being higher than for normal tissue where ADC was $1.32 [0.21] \times 10^{-3} \text{ mm}^2/\text{s}$, and about 1–2 orders of magnitude greater than the values for fat (Thurston, *et al.*, *Science* 286: 2511–2514 (1999)). In addition, size and appearance of lymph nodes varied, especially in the large para-aortic lymph nodes surrounding the inferior *vena cava*. However, mesenteric lymph nodes and Peyer patches were seen in the VEGFR-3-Ig mice.

6. Regression of the developing lymphatic vessels by endothelial cell apoptosis

During embryogenesis, a dramatic increase in K14-driven transgene expression occurs at E14.5, and by E16.5 the expression encompasses the whole embryonic skin (Byrne *et al.*, *Development* 120: 2369–2383 (1994)). When analyzed in the VEGFR-3+/LacZ background by X-Gal staining, the lymphatic networks of the skin were indistinguishable between transgenic and wild-type embryos at E15. At E15.5–16.5, the lymphatic vessels of the transgenic embryos had regressed in some areas. At E17.5, the lymphatic vessels still formed a continuous network but were thinner than in control embryos. At E18.5, the whole cutaneous lymphatic network was disrupted in the transgenic embryos and after birth, none or only a few single disrupted lymphatic vessels were in the skin, mainly accompanying the large dermal blood vessels. Thus, the lymphatic vessels initially form in

the skin during embryogenesis, but regress when the expression of the transgene is turned on. However, the formation of the dermal blood vasculature was not inhibited in the K14-VEGFR-3-Ig embryos as shown by X-Gal staining in the Tie-promoter-LacZ background (Korhonen *et al.*, *Blood* 86: 1828–1835 (1995)).

TUNEL staining was used to detect apoptosis in endothelial cells, which were identified by simultaneous staining for PECAM-1. Apoptotic endothelial cells were seen in the dermis of the transgenic embryos first at E17.5 and E18.5. No endothelial cell apoptosis was seen in wild-type embryos. The TUNEL-positive cells were detected almost exclusively in VEGFR-3 positive endothelia in the transgenic skin, indicating that VEGFR-3-Ig mediated apoptosis was targeted to the lymphatic endothelium.

D. ANALYSIS

The present Example shows that soluble VEGFR-3 fusion protein inhibits lymphangiogenesis and leads to regression of existing fetal lymphatic vessels *in vivo*. Continuous VEGFR-3 signaling is thus essential for the fetal development and maintenance of the lymphatic vascular system.

The absence of lymphatic vessels in the skin of K14-VEGFR-3-Ig mice was associated with a thickening of the dermis and especially the subcutaneous fat layer as in human lymphedema - a disorder caused by insufficiency of the lymphatic system and characterized by swelling of the extremities of increasing severity (Witte *et al.*, Lymphangiogenesis: Mechanisms, significance and clinical implications. in *Regulation of Angiogenesis* (eds. Goldberg, I.D. & Rosen, E.M.) 65–112 (Birkhäuser Verlag, Basel, Switzerland) 1997; Mortimer, *Cancer*, 83: 2798–2802 (1998)). Moreover, the swelling of the feet and increased fluid accumulation in the skin and subcutaneous tissue in the transgenic mice were similar to symptoms of human lymphedema. The skin phenotype of the K14-VEGFR-3-Ig mice thus shares several features with human lymphedema. The results in this Example show that the disruption of VEGFR-3 signaling by the soluble VEGFR-3 protein can almost completely destroy the lymphatic network and lead to a lymphedema-like phenotype. Moreover, as in some cases of lymphedema, the size and appearance of certain regional lymph nodes was variable, indicating that lymph flow and a functional lymphatic vasculature are essential for the formation of normal lymph nodes.

VEGFR-3-Ig also induced regression of the already-formed lymphatics. Thus, inhibition of VEGF-C and/or VEGF-D binding to VEGFR-3 during development leads to apoptosis of the lymphatic endothelial cells and to the disruption of the lymphatic network, which indicates that continuous VEGFR-3 signaling is required for the survival of the lymphatic endothelial cells. In cell culture, VEGFR-3 activates biochemical signaling cascades associated with endothelial cell survival. Although transgenic mice that overexpress either VEGF-C (Jeltsch *et al.*, *Science*, 276: 1423-1425 (1997)) or VEGF-D in the skin develop a hyperplastic dermal lymphatic vasculature, their dermal lymphatic vessels also regress when mated with K14-VEGFR-3-Ig mice. As both VEGFR-3 ligands are also expressed in the skin, the phenotype observed in K14-VEGFR-3-Ig mice might be due to a simultaneous inhibition of both VEGF-C and VEGF-D.

In this study, VEGFR-3-Ig did not seem to affect the blood vessels. The late onset of K14-promoter expression may explain the lymphatic specificity of the VEGFR-3-Ig protein. A substantial increase in K14-promoter activity is not seen until around E14.5–16.5 (Byrne *et al.*, *Development*, 120: 2369-2383 (1994)). Although the expression of endogenous VEGFR-3 is first detected at E8.5 in developing blood vessels, by E14.5–16.5 it has been largely down-regulated in healthy blood vascular endothelia (Dumont *et al.*, *Science* 282, 946–949 1998; Kaipainen, *et al.*, *Proc. Natl. Acad. Sci. USA*, 92: 3566–3570 (1995)). Therefore, during the developmental period when VEGFR-3 no longer occurs normally in the blood vessel endothelium of healthy tissues, VEGFR-3 signaling plays a more minimal role in angiogenesis in the skin than do other receptors.

The data in this example is significant with respect to the patent application in a number of respects. For example, the data demonstrates that soluble VEGFR-3 is a potent and specific inhibitor of lymphangiogenesis *in vivo*, but more broadly, it shows that compounds that can block ligand-mediated VEGFR-3 signalling can modulate the growth of vessels that express VEGFR-3. Also, the data demonstrate that continuous *in vivo* expression of such an inhibitor was not significantly detrimental to the normal growth or activity of the transgenic mice that expressed it during embryonic development, growth into adult mice, and in adulthood. The mice appeared largely normal, except for edema and loss of lymphatics (observed by histological examination) described above, and exhibited no other obvious symptoms of disease.

IV. ANTI-LIGAND ANTIBODIES CAN BLOCK FLT4/LIGAND INTERACTIONS

Attached as Exhibit B is a copy of the journal publication Achen *et al.*, "Monoclonal antibodies to vascular endothelial growth factor-D block its interactions with both VEGF receptor-2 and VEGF receptor-3," *Eur. J. Biochem.*, 267: 2505-15 (2000). I am a co-author of that paper, and I hereby incorporate that paper and the experiments and results reported therein into this declaration by reference. In this paper, we demonstrated that antibodies raised against a ligand for Flt4 -- in this case it was the VEGF-D ligand -- are effective for blocking ligand interactions with the Flt4 receptor.

The data in this paper has relevance to the methods of treatment described and claimed in the patent application because it provides evidence of efficacy for another class of inhibitors, namely, anti-ligand antibodies. While previous examples showed that soluble Flt4 fragments and Flt4 antibodies can inhibit ligand-mediated stimulation of Flt4 *in vivo*, the data in this paper indicates that antibodies to the ligands themselves also can block ligand-mediated stimulation of Flt4.

V. DISCUSSION

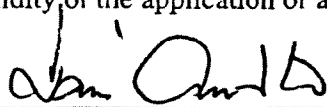
The studies reported above provide scientific evidence that the receptor known as Flt4 (also known as VEGFR-3) and its ligands (VEGF-C and VEGF-D) are involved in lymphangiogenesis in normal and tumor tissues, and involved in angiogenesis in tumor tissues. Also, the data reported herein indicates that where Flt4 and its ligand are involved in tumor-related angiogenesis and/or lymphangiogenesis, compositions that can interfere with ligand-mediated stimulation of Flt4 that is expressed on endothelial cells of tumor vessels can also inhibit tumor growth and/or tumor metastasis. Exemplary compounds for this purpose include circulating Flt4 extracellular domain fragments, which can bind circulating ligand, preventing the ligand from stimulating Flt4 expressed on endothelia; anti-ligand antibodies, which would operate by a similar mechanism; Flt4 antibodies, which can bind Flt4 expressed on endothelial cells and thereby block ligand binding; and any other compounds that bind receptor or ligand and thereby interfere with ligand stimulation of the receptor.

Studies continue to be published reporting the observation of expression of Flt4/VEGFR-3 and/or its ligands (e.g., VEGF-C), in increasing numbers of tumors or tumor vessels. These studies often are done by assaying for Flt4 mRNA or protein using Flt4

polynucleotide probes or anti-Flt4 antibodies as taught in the patent application, and/or polynucleotide or antibodies for the ligand. According to the scientific theory behind the invention, each disease reported in such studies represents a potential disease condition wherein the treatment methods of the patent application would have indications.

Certification

I hereby further declare that all statements made herein of my own knowledge are true and that all statements made on information and belief are believed to be true; and further that these statements were made with the knowledge that willful, false statements and the like so made are punishable by fine or imprisonment, or both under Section 1001 of Title 18 of the United States Code, and that such willful, false statements may jeopardize the validity of the application or any patent issued thereon.



Kari Alitalo

Date: January 31, 2001

Involvement of vascular endothelial growth factor receptor-3 in maintenance of integrity of endothelial cell lining during tumor angiogenesis

Hajime Kubo, Takashi Fujiwara, Lotta Jussila, Hiroyuki Hashi, Minetaro Ogawa, Kenji Shimizu, Masaaki Awane, Yoshiharu Sakai, Arimichi Takabayashi, Kari Alitalo, Yoshio Yamaoka, and Shin-Ichi Nishikawa

Vascular endothelial growth factor (VEGF) plays a major role in tumor angiogenesis. VEGF-C, however, is thought to stimulate the growth of lymphatic vessels because an expression of its specific receptor, VEGF receptor-3 (VEGFR-3), was demonstrated to be restricted to lymphatic vessels. Here we demonstrate that the inactivation of VEGFR-3 by a novel blocking monoclonal antibody (mAb) suppresses tumor growth by inhibiting the neo-angiogenesis of tumor-bearing tis-

suess. Although VEGFR-3 is not expressed in adult blood vessels, it is induced in vascular endothelial cells of the tumor-bearing tissues. Hence, VEGFR-3 is another receptor tyrosine kinase involved in tumor-induced angiogenesis. Micro-hemorrhage in the tumor-bearing tissue was the most conspicuous histologic finding specific to AFL4 mAb-treated mice. Scanning microscopy demonstrated disruptions of the endothelial lining of the postcapillary venule, prob-

ably the cause of micro-hemorrhage and the subsequent collapse of the proximal vessels. These findings suggest the involvement of VEGFR-3 in maintaining the integrity of the endothelial lining during angiogenesis. Moreover, our results suggest that the VEGF-C/VEGFR-3 pathway may serve another candidate target for cancer therapy. (Blood. 2000;96:546-553)

© 2000 by The American Society of Hematology

Introduction

Angiogenesis is essential for tumor progression because it allows oxygenation and nutrient perfusion of the tumor. In the absence of neovascularization, a solid tumor cannot form a large mass.¹⁻³ Angiogenesis is a complex multistep process by which blood vessels are formed from the preexisting vasculature. Previous studies of null mutant mice have demonstrated that development of the embryonic vascular system requires the coordinated expression of various receptor tyrosine kinases (RTKs) and their ligands.⁴ Among these ligands, vascular endothelial growth factor (VEGF) has been shown to play a major role throughout angiogenesis. VEGF action is mediated by 2 RTKs, VEGFR-1 (FLT-1) and VEGFR-2 (FLK-1/KDR), expressed primarily by endothelial cells (ECs). VEGF regulates multiple EC activities such as proliferation, migration, tube formation, and permeability.⁵⁻⁸ Some molecules, such as angiopoietins (Ang1 and Ang2)/Tie2, are implicated in the later stages of vascular development—ie, during vascular remodeling and maturation.⁹⁻¹¹ Based on studies using reagents that neutralize each ligand, it has been suggested that those RTKs involved in the embryonic process are also involved in tumor angiogenesis.¹²⁻¹⁶

Recently, VEGFR-3 was identified as an endothelial-specific RTK related to VEGF receptors.¹⁷ VEGFR-3 is induced in all endothelial cells during early embryogenesis, though its expression eventually disappears from the vascular ECs of adult tissues.¹⁸ In contrast to its transient expression in vascular ECs, VEGFR-3 is expressed constitutively by the adult lymphatic endothelium.¹⁹ VEGF-C, a new member of the platelet-derived growth factor (PDGF)/VEGF family, was first identified as a ligand for VEGFR-

3.²⁰ Among several distinct forms of VEGF-C generated by stepwise proteolysis, the maturely processed VEGF-C could also activate VEGFR-2.²¹ Moreover, another ligand, named VEGF-D²² for VEGFR-3, has been identified recently, illustrating the complex ligand-receptor relationship, which poses a problem for understanding the role of VEGFR-3 during vasculogenesis.

Transgenic overexpression of VEGF-C in the skin has been shown to induce hyperplasia of the lymphatic vasculature (lymph-angiogenesis), leaving the vascular structure unaffected. This observation implies a lymphatic-specific role for VEGF-C/VEGFR-3.^{23,24} Another report using the cornea assay,²⁵ however, demonstrated that VEGF-C could induce angiogenesis of adult tissues. Mice bearing a null mutation of the VEGFR-3 gene display defects in vascular remodeling, indicating a role for VEGFR-3 in angiogenesis.²⁶ Nonetheless, because VEGFR-3 is expressed by vascular ECs in the embryo but not the adult, the role of VEGFR-3 in adult mice is yet to be determined. We generated an antagonistic monoclonal antibody (mAb) against VEGFR-3 to elucidate the role of VEGFR-3 in tumor angiogenesis. We show that VEGFR-3 is indeed involved in tumor angiogenesis and is essential for maintaining the integrity of the endothelial sheet.

Materials and methods

Mice

Six- to 8-week-old nude (nu/nu) mice were purchased from SLC (Shizuoka, Japan). VEGFR-3 null mutant embryos²⁶ were maintained and mated in our animal facility.

From the Departments of Gastroenterological Surgery and Molecular Genetics, Graduate School of Medicine, Kyoto University, Kyoto, and the Laboratory Animal Center, Ehime University School of Medicine, Ehime, Japan; and the Molecular/Cancer Biology Laboratory, Haartman Institute, University of Helsinki, Helsinki, Finland.

Submitted September 13, 1999; accepted March 6, 2000.

Supported by grants from the Japanese Ministry of Education, Science and Culture (07CE2005, 07457085, and 08277102), from the Japanese Ministry of

Health and Welfare, and from the Japan Society for the Promotion of Science Research.

Reprints: Hajime Kubo, Department of Molecular Genetics, Graduate School of Medicine, Kyoto University, Shogoin Kawaharacho 53, Sakyo-ku, Kyoto 606-8507, Japan; e-mail: kuboht@kuhp.kyoto-u.ac.jp.

The publication costs of this article were defrayed in part by page charge payment. Therefore, and solely to indicate this fact, this article is hereby marked "advertisement" in accordance with 18 U.S.C. section 1734.

© 2000 by The American Society of Hematology

Cell culture

The C6 rat glioblastoma cell line (a gift from Dr H. Kataoka, Kyoto University, Kyoto, Japan), the F-2 murine endothelial cell line²⁷ (a gift from Dr K-I Toda, Kyoto University, Kyoto, Japan), and the 293 human embryonic kidney cell line (American Type Culture Collection, Manassas, VA) were grown in Dulbecco's modified Eagle's medium (DMEM; GIBCO/BRL, Grand Island, NY) supplemented with 10% fetal calf serum (FCS) (HyClone Laboratories, Logan, UT). PC-3 human prostate adenocarcinoma cell line (a gift from Dr N. Itoh, Kyoto University, Kyoto, Japan) were maintained in RPMI 1640 medium (GIBCO/BRL) containing 10% FCS.

Gene transfection

For the preparation of Fc chimeric proteins, cells from the 293 cell line were plated on a 100-mm tissue culture dish to reach 70% confluence the next day and were transfected with 15 μ g pCDM8-VEGFR-3-Fc (described below), pCDM8-VEGFR-1-Fc,²⁸ or pCDM8-VEGFR-2-Fc²⁹ plasmid DNA mixed with 25 μ g Trans-IT (Mirus, Madison, WI) according to the manufacturer's instructions. Transfected cells were grown in DMEM/F12 medium, and culture supernatants were harvested 5 days after transfection. Fusion protein was purified using protein G-Sepharose columns (Pharmacia Biotech, Uppsala, Sweden).

Plasmid vector containing murine VEGFR-3 cDNA (P2BIS neo/mFL14¹⁷) was kindly provided by Dr W. I. Wood (Genentech, Cambridge, MA). cDNA containing full-length VEGFR-3 with *Not* I and *Sal* I restriction sites at the 5' and 3' ends, respectively, was obtained from P2RIS neo/mFL14 and subcloned into the expression vector pCDNA3.

Generation of anti-VEGFR-3 monoclonal antibody

A 2.3-kb fragment of murine VEGFR-3 cDNA (positions 45-2354 in the GeneBank L07296), encoding the extracellular domain of VEGFR-3, was subcloned into the expression vector pCDM8-hIgG.²⁹ Rat monoclonal antibodies against VEGFR-3-Fc protein were produced using standard methods as described.²⁹ In brief, an 8-week-old Wistar rat was first immunized subcutaneously with 500 μ g VEGFR-3-Fc protein in complete Freund's adjuvant (Difco, Detroit, MI) and then was administered 3 intraperitoneal shots of 250 μ g VEGFR-3-Fc protein in Freund's incomplete adjuvant (Difco) in alternating weeks and finally was given an intravenous boost of 100 μ g VEGFR-3-Fc protein. Three days after the boost, the spleen cells were harvested and fused with the murine myeloma X63Ag8. Undiluted supernatants from hybridoma were screened by enzyme-linked immunosorbent assay (ELISA) plates coated with 50 ng/mL VEGFR-3-Fc; VEGFR-2-Fc²⁹ and VEGFR-1-Fc were used as controls.²⁸ Positive hybridomas were cloned by the limiting dilution technique and were subcloned twice.

VEGF-C/VEGFR-3 binding inhibition assay by ELISA

The N-terminal signal sequence of mouse stem cell factor (MMU44725; 198-279) and the 5 repeated *myc*-tag sequences were inserted to a 5' end of the cDNA fragment corresponding to the mature VEGF-C (U43142; 705-1052),²¹ which was generated by reverse transcription-polymerase chain reaction amplification of mRNA prepared from PC-3 cells (5-*myc*-VEGF-C). For the binding inhibition study, ELISA plates coated with 50 ng/mL VEGFR-3-Fc protein were first incubated with various dilutions of mAbs and then with the conditioned medium (CM) of 293 cells transfected by the 5-*myc*-VEGF-C gene. Binding with 5-*myc*-VEGF-C was detected by the anti-*myc* tag antibody (9E10) (Santa Cruz Biotechnology, Santa Cruz, CA) and then by horseradish peroxidase (HRP)-conjugated anti-mouse IgG (Zymed, San Francisco, CA). Plate-bound enzymic activity was detected by using 3',3',5',5'-tetramethylbenzidine (Chemco-Sero Therapeutic Research Institute, Kumamoto, Japan), and absorbance of each well was measured using the ELISA reader.

Tumor transplantation

Six- to 8-week-old nude (nu/nu) mice (SLC, Shizuoka, Japan) underwent subcutaneous transplantation of 2×10^6 C6 rat glioblastoma cells or PC-3 prostate cancer cells in 0.1 mL phosphate-buffered saline (PBS) on the right

flank. Subcutaneous injections of mAbs were given on the left flank of mice. Tumor size was measured in 2 dimensions, and the volume was calculated using the formula, width² \times length/2. After 14 days, all mice were humanely killed and autopsied.

Immunohistochemistry

Tissues were fixed in 4% paraformaldehyde in PBS overnight, embedded in paraffin and sectioned at 5 to 7 μ m. The sectioned specimens were incubated first in bleaching solution (methanol, 0.2% Na₂S₂O₈; 0.6% H₂O₂) for 30 minutes at room temperature to block endogenous peroxidase. After rehydration, the sections were blocked by incubation with 1% bovine serum albumin in PBS-0.1% Tween 20 (PBS-T) for 20 minutes at room temperature and then incubated overnight with respective primary antibodies: rat anti-VEGFR-3 mAb, AFL4 (20 μ g/mL); rat anti-VEGFR-2 mAb, AVAS12²⁹ (10 μ g/mL); and rat mAb for murine PECAM-1 (5 μ g/mL, Mec13.3; PharMingen, San Diego, CA). After they were washed 3 times in PBS-T for 10 minutes each at room temperature, the sections were incubated with 1 μ g/mL HRP-conjugated anti-rat IgG(H+L) (Biosource, Camarillo, CA) for 1 hour at room temperature. After washing with 3 exchanges of PBS-T, the enzymatic reaction with enhanced DAB substrate kit (TSA-Indirect; NEN Life Science Products, Boston, MA) was allowed to proceed until the desired color intensity was reached. For immunohistochemical analysis of AFL4-treated mice, tissues were incubated with a biotinylated anti-PECAM-1 antibody (1/100) as a primary antibody, and HRP-conjugated streptavidin (Zymed) (1/1000) was used as a developing reagent.

The densities of PECAM-1⁺ and VEGFR-3⁺ vessels were calculated according to the method described by Gasparini and Harris.³⁰ A minimum of 5 fields ($\times 200$) was counted per slide.

Whole-mount immunostaining was performed according to the protocol previously described.³¹ In some experiments, stained whole-mount specimens were embedded in polyester wax (BDH, Poole, UK) and sectioned.

Scanning electron microscopy (SEM)

Tumor masses with surrounding tissues were dissected carefully and fixed with 3% glutaraldehyde in 0.1 mol/L phosphate buffer (pH 7.4). The method of SEM observation was as previously reported.³² In brief, the specimens were postfixed with OsO₄ and were hydrolyzed with 8N HCl for 25-60 minutes at 60°C. After a brief rinse, the specimens were dehydrated through a graded series of ethanol, immersed in isoamyl acetate, critical-point dried, coated with platinum, and observed with an SEM (Hitachi S-800, Tokyo, Japan).

Western blot analysis

Western blot analysis was performed as described.²⁹ The filter was probed with 2 μ g/mL anti-VEGFR-3 mAb or a control mAb, followed by treatment with HRP-coupled goat anti-rat IgG, and visualized using the enhanced chemiluminescence reagent (NEN Life Science Products).

Phosphorylation assay

F2 cells were grown to subconfluence in DMEM supplemented with 10% FCS. The medium was removed and replaced with fresh DMEM containing 10% FCS with or without antibodies (AFL4, rat IgG fraction 50 μ g/mL) for 15 minutes; this was followed by stimulation with one-fifth diluted VEGF-C CM. Fifteen minutes after VEGF-C stimulation, the cells were lysed in lysis buffer (10 mmol/L Tris-HCl, pH 7.5, 150 mmol/L NaCl, 1 mmol/L EDTA, 1 mmol/L EGTA, 1% NP-40, 0.2 mmol/L PMSF, 0.5 mmol/L sodium vanadate, 2 mmol/L sodium fluoride). VEGFR-3 was immunoprecipitated from cell lysates by protein G-Sepharose after incubation with the anti-VEGFR-3 mAb. Proteins were resolved with sodium dodecyl sulfate-polyacrylamide gel electrophoresis under nonreducing conditions and were probed with HRP-conjugated anti-phosphotyrosine mAb (PY20; Transduction Laboratories, Lexington, KY). Filters were reprobated with anti-VEGFR-3 mAb to measure the amount of protein loaded on each lane.

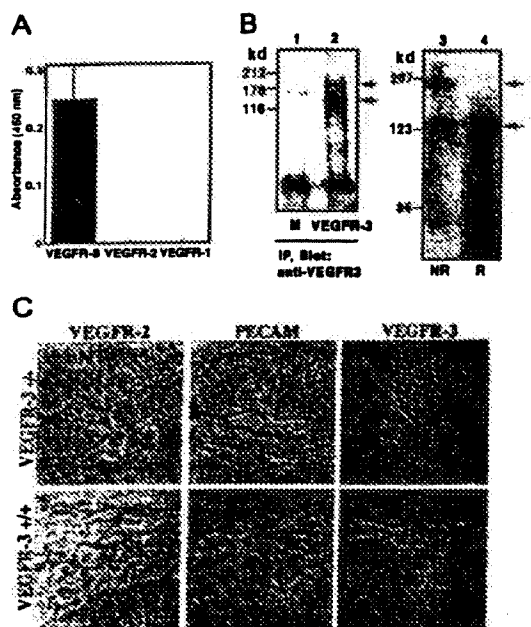


Figure 1. Specificity of AFL4. (A) AFL4 binding to VEGFR-1-Fc, VEGFR-2-Fc, or VEGFR-3-Fc was analyzed by ELISA. The absorbance at 450 nm is depicted. Each bar represents the mean \pm SEM of triplicate assays. (B) Cell lysates from the 293 cell line transiently transfected with murine VEGFR-3 DNA (lane 2) or mock transfected (lane 1, M) were precipitated with AFL4 and immunoblotted with the same antibody. (IP, immunoprecipitation.) Two bands of 195- and 125-kd proteins were detected in lane 2 under reducing conditions. Through immunoblotting of the cell lysates from the murine EC line F2 with anti-VEGFR-3 mAb, 2 bands were detected in nonreducing conditions (NR), whereas only a 125-kd band was seen under reducing conditions (R) (lanes 3, 4). Arrows denote the positions of the unprocessed 195-kd form and the proteolytically processed 125-kd form of VEGFR-3. (C) Specificity of AFL4 in tissue sections. Sagittal sections were prepared from embryonic day 9.5 VEGFR-3^{-/-} or VEGFR-3^{+/+} embryos and stained with AFL4, anti-PECAM-1 mAb, and anti-VEGFR-2 mAb. Arrows indicate blood vessels in the mesenchymal region around the neural tube (NT). Note that all PECAM-1⁺ cells are also VEGFR-2⁺ and VEGFR-3⁺ at this stage of embryonic development.

Results

Production of an antagonistic anti-mouse VEGFR-3 mAb

After screening more than 500 clones, 1 clone, AFL4 (IgG2ak), was isolated as reacting specifically to VEGFR-3-Fc but not to VEGFR-1-Fc or VEGFR-2-Fc (Figure 1A). Two polypeptides were precipitated and immunodetected with AFL4 in cell lysates of VEGFR-3 gene-transfected 293 cells but not from mock-transfected cells (Figure 1B; lanes 1, 2). Through immunoblot analysis of total extracts of the F-2 endothelial cell line,²⁷ 2 bands of 195- and 125-kd were detected with AFL4 (Figure 1B; lane 3) under nonreducing condition, whereas only the 125-kd band was observed under reducing conditions (Figure 1B; lane 4). These results are consistent with the previous observation that a 175-kd precursor of VEGFR-3 matures to a 195-kd form, which is then proteolytically cleaved into the 125-kd and 75-kd fragments,³³ each linked by disulfide bonds.

To further evaluate the specificity of AFL4, serial transverse sections were prepared from E9.5 VEGFR-3^{-/-} or VEGFR-3^{+/+} embryos and immunostained by AFL4. The AFL4 immunostaining was seen in the vascular endothelial lining of the wild-type embryo but not in that of the VEGFR-3^{-/-} embryo, whereas the expression

of VEGFR-2 and PECAM-1 was detected in both groups (Figure 1C). From these results, we concluded that AFL4 is specific to VEGFR-3 and can be used for various purposes, including immunoprecipitation, immunoblotting, and immunostaining of fixed tissues.

We next investigated whether AFL4 blocks the function of VEGFR-3. AFL4 could block the binding of myc-tagged VEGF-C to ELISA plates coated with VEGFR-3-Fc, whereas anti-VEGFR-2 mAb (AVAS12)²⁹ could not, indicating that AFL4 recognizes the ligand-binding site of VEGFR-3 (Figure 2A). Although these analyses did not permit a precise determination of the binding affinity of AFL4 for VEGFR-3, the IC₅₀ for AFL4 inhibition of VEGF-C binding to VEGFR-3 was estimated to be 0.5 μ g/mL. We also examined whether the blocking of ligand binding leads to the suppression of receptor signaling. We stimulated F2 cells by VEGF-C in the presence of AFL4 or AVAS12. Tyrosine phosphorylation of immunoprecipitated VEGFR-3 was measured by anti-phosphotyrosine mAb. Compared with the control, AFL4 treatment resulted in 6- and 3-fold reduction of VEGF-C-induced tyrosine phosphorylation at 125-kd and 195-kd bands, respectively (Figure 2B).

Lymphatic specific expression of VEGFR-3 protein in adult mouse

Although a previous study¹⁸ and Figure 2 demonstrated VEGFR-3 expression in the vascular EC of early embryos, AFL4 recognized only lymphatic vessels in later life. Figure 3 showed the whole-mount immunostaining of the mesentery of E17 embryos, in which lymphatic vessels easily could be distinguished morphologically from vein and artery running in parallel (Figure 3A-C). In cross-sections, staining could be found only in the endothelial cells of the lymphatic vessels that did not contain blood cells in the lumen (Figure 3D).

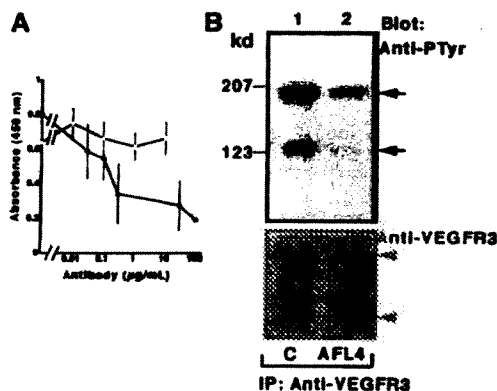
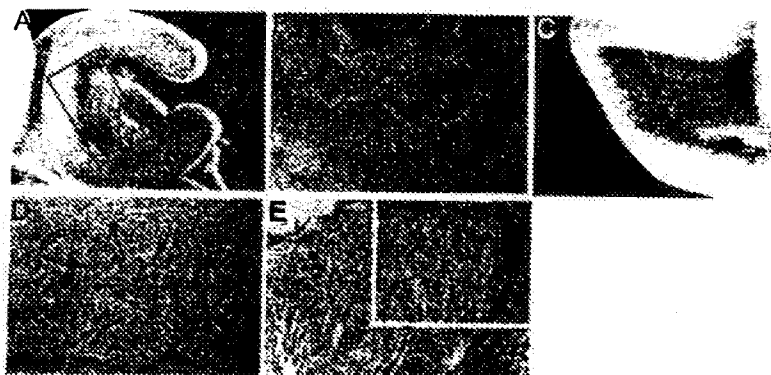


Figure 2. AFL4 blocks VEGFR-3 function by inhibiting VEGF-C binding. (A) Inhibition of binding of VEGFR-3 to VEGF-C by AFL4. Culture supernatant of 293 cells transfected with 5 myc-tagged VEGF-C DNA was incubated with various doses of AFL4 (●) or anti-VEGFR-2 mAb (○) and added to microtiter plates coated with mVEGFR-3-Fc. Binding was quantified by using the anti-myc mAb as a primary antibody, and absorbance at 450 nm was determined. Data indicate the background-corrected mean \pm SEM from triplicate wells. (B) Tyrosine phosphorylation of VEGFR-3 in F2 cells was induced by VEGF-C CM in the presence of control IgG (lanes 1, 3) or AFL4 (lanes 2, 4). Total cell lysates were immunoprecipitated with anti-VEGFR-3 mAb and subjected to serial immunoblotting with anti-phosphotyrosine antibody (upper) and anti-VEGFR-3 mAb (lower). Arrows and arrowheads denote the positions of 195-kd and 125-kd forms of VEGFR-3. Relative density of bands against 125-kd bands of the control lanes (lane 1, upper and lower panels) were 195-kd/125-kd 3.7/1 (lane 1, upper), 0.8/0.2 (lane 2, upper), 0.78/1 (lane 1, lower), and 0.6/1.1 (lane 2, lower). Reduction ratios after correction by the amount of protein were 0.32 and 0.18 for 195-kd and 125-kd bands, respectively.

Figure 3. Lymphatic-specific expression of VEGFR-3 in embryonic day 17 (E17) embryos and adult dermis. (A) Whole-mount staining of the mesentery of E17 embryos by AFL4. A fraction of vascular system is stained. (B) Higher magnification of the marked area in panel A demonstrates that lymphatic vessels with typical sac-like structure are stained (arrows). (C) PECAM-1 staining of the same region shows that blood vessels (arrow) and lymphatic vessels (arrowhead) are stained. (D) A section of the E17 mesentery illustrating stained endothelial vessel (arrow) and an unstained blood vessel (arrowhead) ($\times 200$). Note that all stained vessels do not contain hematopoietic cells. (E) A section of an adult skin illustrates VEGFR-3⁺ (arrows) and VEGFR-3⁻ vessels ($\times 100$). Higher magnification (inset, $\times 200$) reveals that VEGFR-3⁺ vessels (arrows) do not contain hematopoietic cells, whereas unstained blood vessels do (arrowheads).



We next examined VEGFR-3 expression in adult cutaneous tissues. Cells lining the luminal wall of a vascular structure (indicated by arrows) were immunostained by AFL4 (Figure 3E). In contrast to the lack of reactivity to blood vessels containing hematopoietic cells (indicated by arrowheads), all AFL4-reactive vessels did not contain blood cells, suggesting lymphatic specific expression of VEGFR-3. This staining pattern corroborates well with previous *in situ* analysis showing that VEGFR-3 is specific to ECs lining the lymphatic vessels.¹⁸

To determine the role of VEGFR-3 in the maintenance of the adult lymphatic system, 1 mg AFL4 was injected subcutaneously into 8-week-old mice on alternating days for up to 3 weeks. During this 3-week period of continuous AFL4-injection, we could not detect any gross abnormality in the treated mice compared with the control mice, which were treated with non-antagonistic anti-VEGFR-2 mAb or PBS (data not shown). Thus, VEGFR-3 appeared not to be essential for the maintenance of the adult lymphatic system.

AFL4 suppresses the growth of xenogenic tumors in nude mice

The antagonistic anti-VEGFR-3 mAb enabled us to examine the involvement of VEGFR-3 in tumor-induced neo-angiogenesis. For this purpose, we first used the C6 glioblastoma cell line, which grows aggressively in the nude mouse.³³ C6 cell line has been shown to secrete VEGF³⁴ and VEGF-C.³⁵

To determine the effect of AFL4 treatment on the C6 growth, 200, 600, or 1000 μ g purified AFL4 was injected on alternating days for 12 days into mice grafted with 2×10^6 C6 tumor cells. As controls, 600 μ g AVAS12, nonantagonistic anti-VEGFR-2 mAb

was injected in the same manner. The size of tumor was measured from day 5 to day 14 after the tumor transplantation. As shown in Figure 4A and Table 1, AFL4 treatment inhibited tumor growth at all doses. Because 200 μ g showed less effect than other doses, we decided to use 600 μ g for subsequent experiments.

To determine the timing of VEGFR-3 involvement in tumor progression, 3 protocols for antibody injection were tested: (1) day 0 to day 12, (2) day 0 to day 6, and (3) day 7 to day 13. The continuous injection of AFL4 suppressed tumor growth by approximately 75%. Because the discontinuation of treatment on day 7 (protocol 2) resulted in the prompt recovery of tumor growth, it is likely that VEGFR-3 is continuously required for tumor growth (Figure 4B). We also attempted to determine whether growth was suppressed if AFL4 injection was commenced from day 7 (protocol 3, Figure 4C). Although we did observe a reduction of tumor size, the effect of this protocol was not statistically significant ($P = .06$).

To examine whether AFL4 treatment suppresses the growth of other tumor types, a human prostatic cancer cell line, PC-3 was used. PC-3 cells were reported to secrete VEGF-C.²⁰ PC-3 cells grew more slowly than C6 cells in the subcutaneous region of the nude mice. At day 14, PC-3 tumors reached an average size of 291 ± 90.1 mm³ in control mice (Table 1), whereas we could not detect PC-3 tumor mass at day 14 in AFL4-treated mice (Table 1).

Induction of VEGFR-3 expression during tumor-induced angiogenesis

Such a dramatic suppression of tumor growth by AFL4 treatment implicates the role of VEGFR-3 in angiogenesis rather than in the formation of lymphatic vessels, though VEGFR-3 is not expressed

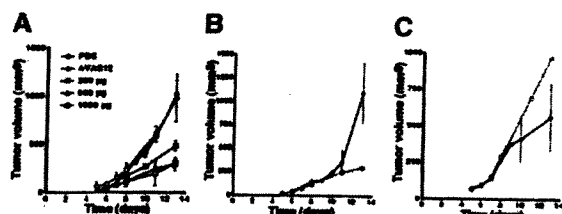


Figure 4. Anti-VEGFR-3 suppresses the growth of C6 tumor cells implanted subcutaneously in nude mice. (A) Protocol 1: days 0 to 12. Alternate-day treatment with PBS ($n = 8$), anti-VEGFR-2 (600 μ g/dose; $n = 4$), or anti-VEGFR-3 (200 μ g/dose, 600 μ g/dose, 1000 μ g/dose; $n = 4$ each). Tumor size at day 14 was summarized in Table 1. (B) Protocol 2: days 0 to 6. Injection of anti-VEGFR-3 treatment (600 μ g/dose, closed circle; $n = 4$), compared with continuous injection (days 0-12) (open circle; $n = 4$). (C) Protocol 3: days 7 to 13. Anti-VEGFR-3 treatment (600 μ g/dose, closed circle; $n = 4$) and PBS treatment (open circle; $n = 4$). The growth curves of tumors in PBS-treated mice were used as reference points for each figure.

Table 1. Suppression of tumor growth by AFL4 treatment

Antibodies	μ g/dose	Tumor volume (mm ³) \pm
C6 tumor*		
PBS	—	982 \pm 246
Avas12†	600	1027 \pm 137
AFL4	200	488 \pm 58.5§
	600	296 \pm 67.0§
	1000	312 \pm 38.4§
PC-3 tumor		
Avas12†	600	291 \pm 90.1
AFL4	600	Not detectable

Experimental procedures were as described in Figure 4.

*Results using the C6 glioblastoma cell line are the same as those presented in Figure 4.

†AVAS12 is a nonblocking mAb to mVEGFR-2.

‡Each value represents mean \pm SEM of 8 mice for the PBS-treated group and 4 mice for other groups.

§ $P < .01$.

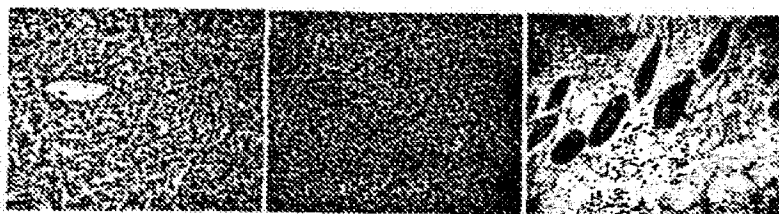


Figure 5. Induction of VEGFR-3 expression during tumor-induced angiogenesis. Immunostaining for VEGFR-3 (A) and PECAM-1 (B) in adjacent sections of C6 subcutaneous tumors (day 7) in nude mice ($\times 200$). Intratumoral VEGFR-3⁺ (A, arrows) containing blood cells are also positive for PECAM-1 expression (B, arrows). Note that hemorrhages are not conspicuous at this stage. (C) Immunostaining for VEGFR-3 in a section of C6 tumors with surrounding tissues ($\times 100$). Note the presence of VEGFR-3⁺ (black arrows) and VEGFR-3⁻ (white arrows) vessels, both containing hematopoietic cells. Arrowheads indicate VEGFR-3⁺ vessels that do not contain hematopoietic cells. Asterisk indicates the edge of a tumor.

in the blood vessels of normal tissues. Thus, we hypothesized that VEGFR-3 expression might be induced by tumor transplantation in the surrounding tissue. To test this possibility, we investigated VEGFR-3 expression in the tumor-bearing tissues. Sections of tumor and surrounding tissues were immunostained with AFL4 or anti-PECAM-1 mAb. VEGFR-3 expression was detected in intratumoral vessels (indicated by arrows) (Figure 5A). Unlike normal tissues (Figure 3E), VEGFR-3⁺ vessels in this section contained blood cells, indicating that VEGFR-3 expression was induced in the tumor blood vessels. A similar staining pattern was seen for PECAM-1 staining of serial sections, demonstrating EC-specific expression of VEGFR-3 (Figure 5B). It should be noted, however, that not all EC in the tumor vessels expressed VEGFR-3. Intratumoral VEGFR-3⁺ vessel density, including lymphatics, was 30 ± 1.2 per high-power field, whereas that of normal skin tissue was 7.4 ± 0.3 per high-power field. Because the intratumoral PECAM-1⁺ vessel density was 92 ± 2.8 , approximately 30% of intratumoral vessels become activated to express VEGFR-3⁺, and because PECAM-1⁺ vessel density in the normal skin was 38 ± 1.3 , the intratumor region was indeed rich in blood vessels.

VEGFR-3 staining was also induced in vessels surrounding the tumor (Figure 5C).

Histologic basis for tumor suppression in AFL4-treated mice

To gain insight into the VEGFR-3-dependent cellular processes during tumor-induced angiogenesis, we compared the vascular system surrounding tumors of AFL4-treated and control mice. In the control mouse, the size of the vascular trunk supplying branches to tumors was larger than the corresponding trunk in the tumor-free side of skin, suggesting an increase of overall blood flow in the tumor-bearing side (Figure 6A). As expected from the reduced tumor size in AFL4-treated mice, the vascular trunk governing tumor blood supply was smaller than that of the control mice (Figure 6B). In control mice, several branches of similar size stemmed from this trunk, which further divided into smaller branches (Figure 6A,C). In contrast, though the primary branches were detectable in the AFL4-treated mice, their sizes were variable, and they did not develop the fan-like architecture found in the control tumor (Figure 6B,D). Secondary and tertiary branches appeared to be very thin. Many micro-hemorrhages were found



Figure 6. AFL4 treatment inhibits tumor angiogenesis. Tumor-bearing regions were photographed on day 14 after tumor transplantation. Gross appearance of representative vascularization of control (A) and AFL4-treated (B) mice. Arrows and arrowheads indicate the vascular trunks governing tumor blood supply and those of the tumor-free side, respectively. Note that the size of the trunk is larger on the tumor-bearing side than on the other side. Such a dilatation is not clearly seen in the AFL4-treated mouse. (C, D) Higher magnification than that in A and B, respectively. Secondary and tertiary branches are poorly developed in the AFL4-treated mouse. Note the many micro-hemorrhages in this AFL4-treated tumor (arrows). Asterisks indicate tumors.

along the small branches (Figure 6B,D). Although massive bleeding was frequently found in the necrotic regions of tumors in the control mice, micro-hemorrhages were rare. This macroscopic observation was confirmed by microscopic analysis. Control tumor sections stained with hematoxylin–eosin showed enlarged vessels surrounding tumors (data not shown), whereas overall vascularity around the tumors was lower in the AFL4-treated group (data not shown). Moreover, the number of PECAM-1⁺ EC within the tumor mass was reduced to 40% in the control group (Figure 7A,B,E). Conversely, 4 times more micro-hemorrhagic regions were detected in the AFL4-treated group (Figure 7C,D,F).

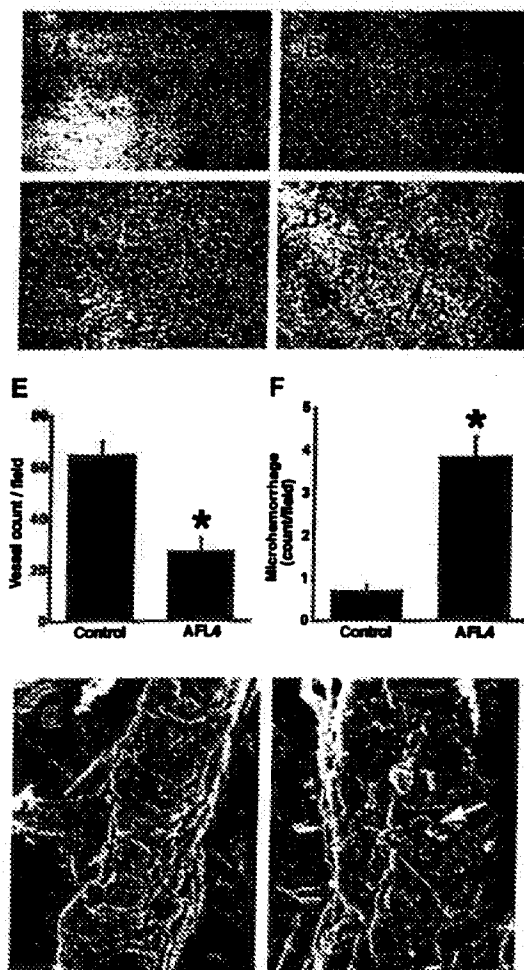


Figure 7. Histology of intratumor vasculatures. (A, B) Tumor vasculatures are visualized by anti-PECAM-1 immunostaining. Micrographs are of representative sections prepared from the control (A) and AFL4-treated mice (B) ($\times 200$). (C, D) Representative H&E-stained tumor sections from controls (C) and anti-VEGFR-3-treated mice (D) ($\times 200$). In anti-VEGFR-3-treated tumors, many micro-hemorrhages are observed (arrows). (E) Vessel counts per field were determined from at least 5 different vision fields of sections from control ($n = 4$; 85 ± 5.2 /high-power field) and AFL4-treated mice ($n = 4$; 27.5 ± 5.3 /high-power field) ($\times 200$). Data are plotted as mean \pm SEM. $^*P < .01$. (F) The number of micro-hemorrhages was scored in high-power fields ($\times 200$) of H&E-stained tumor sections (at least 5 different vision fields each of 4 tumors). Control, 0.73 ± 0.13 /high-power field; AFL4, 3.9 ± 0.46 /high-power field. Data are plotted as mean \pm SEM. $^*P < .01$. Statistical differences between groups were computed using the Student *t* test. (G) Representative SEM of a postcapillary venule in control tumors ($\times 3800$). (H) SEM of a postcapillary venule in anti-VEGFR-3-treated tumors reveals disruption of the endothelial sheet, exposing red blood cells (arrow) ($\times 2200$).

To determine the morphologic basis of the micro-hemorrhage in the AFL4-treated tissues, the vessels connecting to the tumor were analyzed systemically by SEM. We could not detect any abnormalities in the morphology of the proximal vessels of AFL4-treated mice, suggesting that these vessels developed normally (data not shown). However, at the level of postcapillary venules, disruption of the endothelial lining was observed frequently in AFL4-treated mice (Figure 7G,H). Erythrocytes could be seen through the cleft. The formation of such clefts was barely detectable in the postcapillary venule surrounding the tumors in control mice.

Discussion

In this study we established an antagonistic mAb to VEGFR-3 (AFL4) and used AFL4 to evaluate the role of this RTK in tumor angiogenesis. Although VEGFR-3 is not expressed in the vascular EC of adult mice, our result showed that VEGFR-3 expression is induced in the vascular EC upon the implantation of tumor cells. Furthermore, the growth of C6 glioma cells and PC-3 prostate carcinoma cells was suppressed by the injection of AFL4, presumably because of the inhibition of the establishment of the vascular architecture in tumor-bearing tissues. Taking the previous study on VEGFR-3^{-/-} embryos²⁶ into account, besides embryonic angiogenesis, VEGFR-3 is involved in the neo-angiogenesis of adult tissue.

Sustained AFL4 treatment resulted in no gross anomalies in normal mice. Thus, during the 3 weeks of mAb injection, the architecture of the lymphatics and the vascular system remained unaffected in the absence of VEGFR-3 function; however, the effect over a longer period of time remains to be investigated. Recently, it has been demonstrated that the prolonged suppression of VEGF activity in the adult mouse has no effect on the maintenance of the vascular system, though it suppresses angiogenesis in the newborn mouse.³⁶ The fully established lymphatic and vascular systems are basically resistant to treatment with various reagents that suppress neo-angiogenesis. Because of the neo-angiogenesis-specific effect of these reagents, this approach has been expected to be chosen for cancer therapy. Our current results demonstrate clearly that VEGFR-3 is a potentially useful molecule for targeting in future cancer therapy.

Compared with the phenotype of VEGFR-2^{-/-} mice, in which formation of the primitive vascular plexus is impaired,³⁷ it has been indicated that VEGFR-3 is involved at a later stage of vascular development, particularly in the remodeling of the primitive plexus to a higher-order architecture.²⁶ The absence of secondary and tertiary branches in AFL4-treated mice suggests a VEGFR-3 role in the remodeling of tumor-induced neo-angiogenesis. Angiopoietins/Tie-2 has also been implicated in the remodeling process of embryonic and tumor-induced angiogenesis. It is likely that the molecular requirements for vascular development in the embryo and for tumor-induced neo-angiogenesis are essentially the same and involve an ordered expression of multiple tyrosine kinase receptors.

Which process of angiogenesis is affected by the inhibition of VEGFR-3? Although the role of VEGFR-3 in the remodeling of vascular formation has been implicated, these reports did not specify the process beyond the word *remodeling*.²⁶ This may be, in part, because of an inherent difficulty in studying embryonic angiogenesis in which angiogenesis proceeds asynchronously according to region-specific timetables. In other words, various

intermediate steps of angiogenesis are mixed within an embryo. In contrast, tumor-induced angiogenesis is a synchronous process that can be induced in a relatively homogeneous microenvironment. Moreover, the progression of angiogenesis during tumor growth has been described in detail. With these considerations in mind, we attempted to obtain insight into the histologic basis of the phenotype induced by AFL4-injection. Although AFL4 treatment appeared to be identical to other anti-angiogenic reagents in that it inhibited the supply of vascular branches to the tumor, we demonstrated that micro-hemorrhage, presumably because of the disruption of the endothelial lining at the postcapillary venule level, is a characteristic feature of AFL4-treated tissues. It is difficult to rule out the possibility that this effect is caused by the cytotoxic reaction of AFL4 to VEGFR-3⁺ EC, but we prefer to think that this disruption is derived from the blockage of VEGFR-3 function. This histologic sign has not been described in previous experiments in which other RTKs are blocked. Because micro-hemorrhages are too conspicuous to be overlooked, frequent micro-hemorrhages may be specific to VEGFR-3 inhibition.

How VEGFR-3-block caused the disruption of endothelial structure is difficult to specify. According to previous studies, sprouting of EC occurs only at the levels of capillaries, postcapillary venules, and precapillary arterioles, where no smooth muscle is present.³⁸ By the repeated sprouting, splitting, and anastomosis of blood vessels at this level, the overall peripheral vascular bed in the tumor-bearing tissues increases. This increase in the vascular bed contributes to the reduction of regional vascular resistance, thereby resulting in the increased blood supply. The change of blood supply induces restructuring of the more proximal vessels connecting to tumor, as observed in the current study. Because the angiopoietins/Tie2 signal was shown to regulate interactions between ECs and smooth muscle cells,⁹⁻¹¹ it is conceivable that this signal is required for vascular remodeling in which the distal blood vessel is restructured to the more proximal form associated with smooth muscles. In the Tie2-block experiment, however, micro-

hemorrhages in tumor-bearing tissues has not been indicated. Hence, failure in interaction between ECs and smooth muscle cells may not lead to disruption of the endothelial structure.

The frequency of micro-hemorrhages found in AFL4 treated-mice suggests that AFL4 treatment inhibits maintenance of the integrity of the endothelial sheet during angiogenesis. Although further cell biology studies are required for an understanding of the underlying mechanisms, the presence of mural cells at the level of precapillary arterioles and postcapillary venules of AFL4-treated mice suggests that it may not result from inhibition of the interaction between EC and smooth muscle cells. It has been suggested that vascular permeability is increased at the site of tumor-induced angiogenesis. Thus, it is likely that the endothelial lining is agitated during neo-angiogenesis. Indeed, sprouting and pruning would imperil the integrity of the endothelial lining. Yet, micro-hemorrhage is not a frequent outcome of neo-angiogenesis, indicating that regulatory mechanisms maintain the integrity of the endothelial sheet even during dynamic restructuring of the vascular system. Therefore, we speculate that in the process of sprouting and pruning, during which integrity of the EC layer is disturbed, additional signals such as VEGFR-3 may be required for quick restoration of the EC sheet that otherwise leads to the formation of irreparable clefts. If such clefts causing micro-hemorrhage are generated during neo-angiogenesis, the rheologic resistance of the vascular system should increase, thereby resulting in the collapse of more proximal vessels as observed in the AFL4-treated mouse.

Acknowledgments

We thank Dr W. I. Wood (Genentech) for VEGFR-3 cDNA, Dr K. I. Toda for the F-2 cell line, and Dr N. Itoh for the PC-3 cell line. We also thank Drs H. Kataoka, M. Hirashima, and H. Yoshida for their helpful advice, and we thank Dr S. Fraser for critical reading of the manuscript.

References

- Folkman J. What is the evidence that tumors are angiogenesis dependent? *J Natl Cancer Inst*. 1990;82:4.
- Folkman J. Angiogenesis and tumor growth [letter]. *N Engl J Med*. 1996;334:920.
- Hanahan D, Folkman J. Parameters and emerging mechanisms of the angiogenic switch during tumorigenesis. *Cell*. 1996;86:353.
- Hanahan D. Signaling vascular morphogenesis and maintenance. *Science*. 1997;277:48.
- Connolly DT. Vascular permeability factor: a unique regulator of blood vessel function. *J Cell Biochem*. 1991;47:219.
- Carmeliet P, Ferreira V, Breier G, et al. Abnormal blood vessel development and lethality in embryos lacking a single VEGF allele. *Nature*. 1996;380:435.
- Ferrara N, Carver-Moore K, Chen H, et al. Heterozygous embryonic lethality induced by targeted inactivation of the VEGF gene. *Nature*. 1996;380:439.
- Mustonen T, Alitalo K. Endothelial receptor tyrosine kinases involved in angiogenesis. *J Cell Biol*. 1995;129:895.
- Sato TN, Tozawa Y, Deutsch U, et al. Distinct roles of the receptor tyrosine kinases Tie-1 and Tie-2 in blood vessel formation. *Nature*. 1995;376:70.
- Davis S, Aldrich TH, Jones PF, et al. Isolation of angiopoietin-1, a ligand for the TIE2 receptor, by secretion-trap expression cloning. *Cell*. 1996;87:1181.
- Suri C, Jones PF, Patan S, et al. Requisite role of angiopoietin-1, a ligand for the TIE2 receptor, during embryonic angiogenesis. *Cell*. 1996;87:1171.
- Kim KJ, Li B, Winer J, et al. Inhibition of vascular endothelial growth factor-induced angiogenesis suppresses tumor growth in vivo. *Nature*. 1993;362:841.
- Lin P, Polverini P, Dewhirst M, Shan S, Rao PS, Peters K. Inhibition of tumor angiogenesis using a soluble receptor establishes a role for Tie2 in pathologic vascular growth. *J Clin Invest*. 1997;100:2072.
- Millauer B, Shawver LK, Plate KH, Risau W, Ullrich A. Glioblastoma growth inhibited in vivo by a dominant-negative Flk-1 mutant. *Nature*. 1994;367:576.
- Millauer B, Longhi MP, Plate KH, et al. Dominant-negative inhibition of Flk-1 suppresses the growth of many tumor types in vivo. *Cancer Res*. 1996;56:1615.
- Borgstrom P, Hillan KJ, Sriramamo P, Ferrara N. Complete inhibition of angiogenesis and growth of microtumors by anti-vascular endothelial factor neutralizing antibody: novel concepts of angiostatic therapy from intravital videomicroscopy. *Cancer Res*. 1996;56:4032.
- Finnerty H, Kelleher K, Morris GE, et al. Molecular cloning of murine FLT and FLT4. *Oncogene*. 1993;8:2293.
- Willing J, Eichmann A, Christ B. The avian VEGF receptor homologues Quack1 and Quack2 during quail embryonic development: expression in blood-vascular and lymphatic endothelial and non-endothelial cells. *Cell Tissue Res*. 1997;288:207.
- Kaupainen A, Korhonen J, Mustonen T, et al. Expression of the fms-like tyrosine kinase FLT4 gene becomes restricted to endothelium of lymphatic vessels during development. *Proc Natl Acad Sci U S A*. 1995;92:3566.
- Joukov V, Pajusola K, Kaupainen A, et al. A novel vascular endothelial growth factor, VEGF-C is a ligand for Flt-4 (VEGFR-3) and KDR (VEGFR-2) receptor tyrosine kinases. *EMBO J*. 1996;15:290.
- Joukov V, Sorsa T, Kumar V, et al. Proteolytic processing regulates receptor specificity and activity of VEGF-C. *EMBO J*. 1997;16:3898.
- Achen MG, Jeltsch M, Kulk E, et al. Vascular endothelial growth factor D (VEGF-D) is a ligand for the tyrosine kinases VEGF receptor 2 (Flk1) and VEGF receptor 3 (Flt4). *Proc Natl Acad Sci U S A*. 1996;95:548.
- Jeltsch M, Kaupainen A, Joukov V, et al. Hyperplasia of lymphatic vessels in VEGF-C transgenic mice. *Science*. 1997;276:1423.
- Oh SJ, Jeltsch MM, Birkenhager R, et al. VEGF and VEGF-C: specific induction of angiogenesis and

- lymphangiogenesis in the differentiated avian chorio-allantoic membrane. *Dev Biol*. 1997;188:96.
25. Cao Y, Linden P, Farnebo J, et al. Vascular endothelial growth factor C induces angiogenesis in vivo. *Proc Natl Acad Sci U S A*. 1998;95:14389.
 26. Dumont DJ, Jussila L, Taipale J, et al. Cardiovascular failure in mouse embryos deficient in VEGF receptor-3. *Science*. 1998;282:946.
 27. Toda K, Tsujoka K, Maruguchi Y, et al. Establishment and characterization of a tumorigenic murine vascular endothelial cell line (F-2). *Cancer Res*. 1990;50:5526.
 28. Hirashima M, Kataoka H, Nishikawa S, Matsuyoshi N, Nishikawa S-I. Maturation of embryonic stem cells into endothelial cells in an in vitro model of vasculogenesis. *Blood*. 1999;93:1253.
 29. Kataoka H, Takakura N, Nishikawa S, et al. Expression of PDGF receptor alpha, c-Kit and Flk1 genes clustering in mouse chromosome 5 define distinct subsets of nascent mesodermal cells. *Dev Growth Differ*. 1997;39:729.
 30. Gasparini G, Harris A. Clinical importance of the determination of tumor angiogenesis in breast carcinoma: much more than a new prognostic tool. *J Clin Oncol*. 1995;13:765.
 31. Yoshida H, Kunisada T, Kusakabe M, Nishikawa S, Nishikawa SI. Distinct stages of melanocyte differentiation revealed by analysis of nonuniform pigmentation patterns. *Development*. 1996;122:1207.
 32. Fujiwara T, Uehara Y. The cytoarchitecture of the medial layer in rat thoracic aorta: a scanning electron-microscopic study. *Cell Tissue Res*. 1992;270:165.
 33. Pajusola K, Aprelikova O, Pelicci G, Welch H, Claesson-Welsh L, Alitalo K. Signaling properties of FLT4, a proteolytically processed receptor tyrosine kinase related to two VEGF receptors. *Oncogene*. 1994;9:3545.
 34. Plate KH, Breier G, Millauer B, Ullrich A, Risau W. Upregulation of vascular endothelial growth factor and its cognate receptors in a rat glioma model of tumor angiogenesis. *Cancer Res*. 1993;53:5822.
 35. Enholm B, Paavonen K, Ristimäki A, et al. Comparison of VEGF, VEGF-B, VEGF-C and Ang-1 mRNA regulation by serum, growth factors, oncoproteins and hypoxia. *Oncogene*. 1997;22:2475.
 36. Gerber HP, Hillan KJ, Ryan AM, et al. VEGF is required for growth and survival in neonatal mice. *Development*. 1999;126:1149.
 37. Shalaby F, Rossant J, Yamaguchi TP, et al. Failure of blood-island formation and vasculogenesis in Flk-1-deficient mice. *Nature*. 1995;378:62.
 38. Horii K, Suzuki M, Tada S, Saito S. In vivo analysis of tumor vascularization in the rat. *Jpn J Cancer Res*. 1990;81:279.

Monoclonal antibodies to vascular endothelial growth factor-D block its interactions with both VEGF receptor-2 and VEGF receptor-3

Marc G. Achen¹, Sally Roufail¹, Teresa Domagala¹, Bruno Catimel¹, Edouard C. Nice¹, Detlef M. Geleick¹, Roger Murphy¹, Andrew M. Scott¹, Carol Caesar¹, Taija Makinen², Kari Alitalo² and Steven A. Stacker¹

¹Ludwig Institute for Cancer Research, Royal Melbourne Hospital, Victoria, Australia; ²Molecular/Cancer Biology Laboratory, Haartman Institute, University of Helsinki, Finland

Vascular endothelial growth factor-D (VEGF-D), the most recently discovered mammalian member of the VEGF family, is an angiogenic protein that activates VEGF receptor-2 (VEGFR-2/Flk1/KDR) and VEGFR-3 (Flt4). These receptor tyrosine kinases, localized on vascular and lymphatic endothelial cells, signal for angiogenesis and lymphangiogenesis. VEGF-D consists of a central receptor-binding VEGF homology domain (VHD) and N-terminal and C-terminal propeptides that are cleaved from the VHD to generate a mature, bioactive form consisting of dimers of the VHD. Here we report characterization of mAbs raised to the VHD of human VEGF-D in order to generate VEGF-D antagonists. The mAbs bind the fully processed VHD with high affinity and also bind unprocessed VEGF-D. We demonstrate, using bioassays for the binding and cross-linking of VEGFR-2 and VEGFR-3 and biosensor analysis with immobilized receptors, that one of the mAbs, designated VDI, is able to compete potently with mature VEGF-D for binding to both VEGFR-2 and VEGFR-3 for binding to mature VEGF-D. This indicates that the binding epitopes on VEGF-D for these two receptors may be in close proximity. Furthermore, VDI blocks the mitogenic response of human microvascular endothelial cells to VEGF-D. The anti-(VEGF-D) mAbs raised to the bioactive region of this growth factor will be powerful tools for analysis of the biological functions of VEGF-D.

Keywords: angiogenesis; inhibitor; lymphangiogenesis; monoclonal antibody; VEGF-D.

The development of blood vessels during embryogenesis and tumourigenesis is dependent on members of the vascular endothelial growth factor (VEGF) family of proteins (reviewed in [1]). For example, VEGF (also known as VEGF-A, vascular permeability factor and VPF) is critical for early vascular development in the embryo [2,3] and is required for vascularization of many tumours [4,5]. VEGF is angiogenic and binds to the cell surface receptor tyrosine kinases VEGFR-1 (Flt1) [6,7] and VEGFR-2 (Flk1/KDR) [8,9], which are specifically expressed on endothelial cells during embryonic and tumour development [10]. VEGFR-2 plays a crucial role in the regulation of both developmental [11] and tumour angiogenesis [12,13]. VEGF-C, which binds to VEGFR-2 and VEGFR-3 (Flt4) [14], is both angiogenic [15,16] and lymphangiogenic [17] and appears to play a role in the development of lymphatic vessels [18]. The effects of VEGF-C on lymphatic vessels are probably mediated by activation of VEGFR-3 [19], a receptor that is expressed on venous endothelial cells during early embryogenesis but subsequently becomes restricted to the endothelial cells of lymphatic vessels [20].

The most recently discovered mammalian member of the VEGF family, VEGF-D (also known as c-fos-induced growth factor or FIGF) [21], activates VEGFR-2 and VEGFR-3 [22]. VEGF-D is angiogenic [23], mitogenic for endothelial cells [22], is expressed at many sites in the developing embryo, including the lung mesenchyme [24,25], and is localized in human tumours (M. G. Achen, R. A. Williams, M. P. Mineleus, G. E. Thornton, K. Stevens, P. A. W. Rogers, F. Cederman, S. Roufail and S. A. Stacker, unpublished observations). Given that VEGF-D activates receptors on vascular and lymphatic endothelial cells, it has been proposed that VEGF-D can stimulate the growth of blood vessels and lymphatic vessels into regions of the developing embryo or into tumours [22]. VEGF-D is initially synthesized as a precursor protein containing N-terminal and C-terminal propeptides in addition to the VEGF homology domain (VHD) [22]. These propeptides are proteolytically cleaved from the VHD during biosynthesis to generate a mature, secreted form consisting of noncovalent dimers of the VHD [24]. The mature form binds both VEGFR-2 and VEGFR-3 with much higher affinity than unprocessed VEGF-D [24].

Specific inhibitors that block the binding of VEGF-D to its receptors would be extremely useful for analysing the contribution of VEGF-D to the development of blood vessels and lymphatic vessels during embryogenesis, tumour growth and other diseases characterized by deregulated angiogenesis, such as rheumatoid arthritis. Here we describe mAbs raised against the bioactive VHD of human VEGF-D. Interestingly, one mAb, VDI, which binds both unprocessed and fully processed VEGF-D, was able to block the interaction of VEGF-D with both VEGFR-2 and VEGFR-3. This indicates that the regions of VEGF-D that interact with these two

Correspondence to M. G. Achen, Ludwig Institute for Cancer Research, Post Office Box 2008, Royal Melbourne Hospital, Victoria 3050, Australia. Fax: +61 3 93413107, Tel.: +61 3 93413155, E-mail: Marc.achen@ludwig.edu.au

Abbreviations: EpoR, erythropoietin receptor; HMVEC, human microvascular endothelial cell; IL-3, interleukin-3; RU, response units; VEGF, vascular endothelial growth factor; VEGFR, VEGF receptor; VHD, VEGF homology domain.

(Received 20 December 1999, revised 17 February 2000, accepted 28 February 2000)

receptors may be very similar. These mAbs will be useful for analysing the biological functions and structure of VEGF-D.

MATERIALS AND METHODS

Expression of derivatives of VEGF-D, VEGF-C, VEGF and VEGF receptors

Human VEGF-D Δ N Δ C, a polypeptide that contains amino acid residues 93–201 of human VEGF-D tagged at the N-terminus with the FLAG octapeptide (IBI/Kodak), and full-length human VEGF-D tagged at the N-terminus with FLAG (VEGF-D-FULL-N-FLAG) were expressed in stably transfected 293-EBNA cells and purified as described elsewhere [24]. In order to express mouse VEGF-D Δ N Δ C, which consists of the VHD of mouse VEGF-D tagged at the N-terminus with FLAG, a DNA fragment encoding residues 97–206 of mouse VEGF-D [21] was amplified from purified mouse VEGF-D cDNA using the oligonucleotide primers 5'-AGCTACGCGTACTTTCTATGACACTGA and 5'-AGCTACGCGTTATTATGAGTATGGATGGCGG and *Pfu* DNA polymerase (Stratagene, La Jolla, CA) according to the manufacturer. The PCR product was digested with restriction enzyme *MluI* and inserted into the expression vector pEFBOSSFLAG (kindly provided by C. McFarlane, Walter and Eliza Hall Institute for Medical Research, Melbourne) at the *MluI* site downstream of DNA encoding the interleukin-3 (IL-3) signal sequence and FLAG. The sequence of the amplified region was confirmed by nucleotide sequencing, which also indicated that the DNA encoding the IL-3 signal sequence, FLAG and the VHD were in the same reading frame. The construction of the expression vector resulted in the insertion of two amino acids, threonine and arginine, between FLAG and the VHD. The expression cassette for the IL-3 signal sequence/FLAG/VHD polypeptide was inserted into the expression vector pApex-3 (kindly provided by S. Squinto, Alexion Pharmaceuticals, New Haven, CT, USA) using restriction enzyme *XbaI* and the resulting construct was used to transiently transfect 293-EBNA cells using Fugene (Boehringer Mannheim). Mouse VEGF-D Δ N Δ C was purified from conditioned cell culture media by affinity chromatography with M2 (anti-FLAG) mAb as described previously [24]. Human VEGF-C Δ N Δ C was expressed and purified as described previously [26], as was mouse VEGF₁₆₄ [27]. Expression and purification of the extracellular domain of mouse VEGFR-2 tagged at the C-terminus with FLAG has been described previously [27]. A chimeric protein consisting of the extracellular domain of human VEGFR-3 and the Fc portion of human IgG₁ (VEGFR-3-Ig) was expressed by transient transfection of 293-EBNA cells with a VEGFR-3-Ig expression plasmid (a kind gift from K. Pajusola, Biotechnology Institute, Helsinki) using Fugene (Boehringer Mannheim, Germany). VEGFR-3-Ig was purified by affinity chromatography with protein A-Sepharose (Pharmacia) according to the manufacturer.

Production of anti-(VEGF-D) mAbs

The mAbs against the VHD of human VEGF-D (VEGF-D Δ N Δ C) were raised in mice. VEGF-D Δ N Δ C was used to immunize female Balb/c mice on day 85 (intraperitoneal), 71 (intraperitoneal) and 4 (intravenous) prior to fusion with mouse myeloma P3X63Ag8.653 (NS-1) cells. For the first two immunizations, approximately 10 μ g of VEGF-D Δ N Δ C in a 1 : 1 mixture of NaCl/P_i and TiterMax adjuvant (#R-1 Research adjuvant, CytRx Corp., Norcross, GA, USA) was injected whereas for the third immunization 35 μ g of VEGF-D Δ N Δ C in

NaCl/P_i was used. Spleen and myeloma cells were fused using 35% polyethylene glycol and mAbs were selected by screening the fusion with VEGF-D Δ N Δ C. mAb isotypes were determined using an Isostrip isotyping kit (Boehringer Mannheim) and mAbs were purified from the culture media of hybridoma cell lines by affinity chromatography with protein G-Sepharose (Amersham Pharmacia Biotech) according to the manufacturer.

Ba/F3 bioassay cell lines

A bioassay was established in which Ba/F3 cells were stably transfected with a chimeric receptor containing the extracellular domain of human VEGFR-3 [28] and the transmembrane and cytoplasmic domains of the mouse erythropoietin receptor [29] (EpoR; kindly supplied by D. Hilton, Walter and Eliza Hall Institute for Medical Research, Melbourne). The chimeric receptor was made by introducing a *Bgl*II restriction enzyme site at the junction of the regions encoding the extracellular and transmembrane domains of the mouse EpoR cDNA using site-directed mutagenesis. Prior to this, a silent mutation was introduced into the EpoR cDNA in a region encoding the cytoplasmic domain of the EpoR to eliminate a naturally occurring *Bgl*II site. The fragment of the EpoR cDNA encoding the transmembrane and cytoplasmic domains, subcloned in plasmid pcDNA1/Amp (Invitrogen), was then ligated at the *Bgl*II site with a PCR product, consisting of DNA encoding the entire extracellular domain of human VEGFR-3, to generate a cDNA encoding a fusion protein consisting of the VEGFR-3 extracellular domain and the transmembrane and cytoplasmic domains of EpoR. The DNA fragment encoding the extracellular domain of human VEGFR-3 had been amplified by PCR using primers 5'-TAGAAAGCTTAATCTAGAGCCACCATGCAGCGGGGCG and 5'-TAGAGGATCCCTCCATGCTGCCCT and ligated as a *Hind*III-*Bam*HI fragment into *Hind*III-*Bgl*II sites of the EpoR plasmid construct. The DNA encoding the chimeric receptor was subcloned into the expression vector pEF-BOS [30] and cotransfected into the Ba/F3 cell line with pgk-Neo (a plasmid containing a neomycin resistance gene under the control of the promoter of the mouse phosphoglycerate kinase-1 gene [31]), at a ratio of 20 : 1. Transfected cells were selected in G418, and a cell line expressing the VEGFR-3-EpoR chimeric receptor (M_r \approx 150 000) was identified by immunoprecipitation and western blot analysis with antihuman VEGFR-3 (Flt4) polyclonal antibody (R & D Systems, Minneapolis, MN, USA). Expression of the chimeric receptor was confirmed by flow cytometry using mAb 9D9 specific for the extracellular domain of human VEGFR-3 [32]. The cell line expressing the receptor was designated Ba/F3-VEGFR-3-EpoR. A line of pre-B cells, designated Ba/F3-VEGFR-2-EpoR, expressing a chimeric receptor containing the extracellular domain of mouse VEGFR-2 and the transmembrane and cytoplasmic domains of the mouse EpoR, was described previously [22,27] as was the parental Ba/F3 cell line [33].

Assay for determining the response of Ba/F3 bioassay cell lines to ligands

Samples of purified human VEGF-D Δ N Δ C were incubated with varying amounts of anti-(VEGF-D) mAbs for 1 h at 4 °C in NaCl/P_i before dilution of the mixtures 1 : 10 with cell culture medium (Dulbecco's modified Eagle's medium containing 10% (v/v) fetal bovine serum, 50 mM L-glutamine, 50 μ g·mL⁻¹ gentamicin, 1 mg·mL⁻¹ G418) deficient in IL-3. The resulting media contained approximately 500 ng·mL⁻¹ of human VEGF-D Δ N Δ C and varying concentrations of the

mAbs. Ba/F3-VEGFR-2-EpoR cells or Ba/F3-VEGFR-3-EpoR cells were then incubated in the media for 48 h at 37 °C. DNA synthesis was then quantified by the addition of 1 µCi of ³H-thymidine and further incubation for 4 h prior to harvesting using an automated cell harvester (Tomtec®, Orange, CT, USA). Incorporated [³H]thymidine was measured by β-counting (Canberra Packard 'Top Count NXT™', scintillation counter, Meriden, CT, USA).

Enzyme immunoassay

Microtitre plates (Linbro/Titertek, ICN Biomedicals, Aurora, OH, USA) were coated with human VEGF-DΔNΔC or human VEGF-CΔNΔC to which purified mAbs were subsequently added and incubated for 2 h at 4 °C, followed by six washes in NaCl/P_i/0.02% Tween 20. Incubation with an antimouse Ig-HRP (Bio-Rad) followed for 1 h at 4 °C. After washing, the assay was developed with an ABTS substrate system (Zymed) and the assay quantified by reading absorbance at 405 nm in a multiwell plate reader (Flow Laboratories).

Immunoprecipitation and Western blot analysis

For immunoprecipitation of metabolically labeled polypeptides, 293-EBNA cells expressing VEGF-D-FULL-N-FLAG or VEGF-DΔNΔC [24] were grown to 50% confluency, washed and incubated in medium deficient in Cys/Met for 30 min. Cells were then labeled for 16 h in medium containing [³⁵S]Cys/Met at 0.20 mCi per ml. VEGF-D derivatives were then immunoprecipitated from the cell culture medium using M2 or anti-(VEGF-D) mAbs and protein G-Sepharose, subjected to SDS/PAGE and visualized with a phosphorimager (Molecular Dynamics, Sunnyvale, CA, USA). For immunoprecipitation of VEGFR-3-EpoR chimeric receptor, 1×10^6 Ba/F3-VEGFR-3-EpoR cells were lysed in 1 mL of 1% Triton X-100, 10 mM Tris/HCl, pH 8.0, 150 mM NaCl including protease inhibitors (Complete™ protein inhibitor cocktail; Boehringer Mannheim) for 20 min at 4 °C. Affinity purified goat antihuman VEGFR-3 polyclonal antibody was added to a concentration of 2 µg·mL⁻¹ of lysate and the mixture incubated at 4 °C for 2 h. The sample was then incubated with protein A-Sepharose for 30 min at 4 °C, washed three times in 25 mM Tris/HCl, pH 8.0, 150 mM NaCl, 0.1% Triton X-100, twice in 25 mM Tris/HCl, pH 8.0, 150 mM NaCl and once in 50 mM Tris/HCl, pH 8.0, before brief centrifugation, boiling in 2 × SDS/PAGE sample buffer and analysis by SDS/PAGE [34]. Non-radioactive human and mouse VEGF-DΔNΔC were immunoprecipitated with anti-(VEGFD) mAbs or M2 mAb from DMEM containing 10% fetal bovine serum using protein A-Sepharose. For western blotting, proteins were transferred to membrane and probed with antihuman VEGFR-3 polyclonal antibody (for detection of VEGFR-3-Ig chimeric receptor), anti-(VEGF-D) mAbs or biotinylated M2 (anti-FLAG) mAb (IBI/Kodak) (for detection of VEGF-DΔNΔC), followed by horseradish peroxidase conjugated donkey anti-(goat IgG) Ig (Silenus, Australia), or horseradish peroxidase conjugated goat anti-(mouse IgG) Ig (Bio-Rad Laboratories) or peroxidase-conjugated streptavidin (Boehringer Mannheim). Signals were detected using chemiluminescence (ECL, Amersham).

Biosensor analysis

Kinetic analysis. All protein preparations were analysed for homogeneity and buffer exchanged into the appropriate buffers

by micropreparative size exclusion HPLC using a Superose 12 (3.2/30) column installed in a SMART™ system (Amersham Pharmacia Biotech) immediately prior to use [35]. VEGFR-2-FLAG, VEGFR-3-Ig and anti-(VEGF-D) mAbs were coupled to the carboxymethylated dextran layer of a CM5 sensor chip using standard amine coupling chemistry [35] for analysis of ligand binding using a BIAcore 3000 optical biosensor (BIAcore). Automatic targeting of immobilization levels was achieved using BIAcore 3.1 control software [36]. Following immobilization, residual activated ester groups were blocked by treatment with 1 M ethanolamine hydrochloride pH 8.5 followed by washing with 10 mM diethylamine to remove noncovalently bound material. The 10 mM diethylamine was also used to regenerate the sensor surface between analyses. Samples for assay were diluted in running buffer (10 mM Hepes, pH 7.4, 150 mM NaCl, 3.4 mM EDTA, 0.005% Tween 20). The integrity of the surface was assessed by binding of purified mouse VEGF₁₆₅ and human VEGF-DΔNΔC. For antibody inhibition studies, samples of purified human VEGF-DΔNΔC (50 nM) were incubated with varying amounts (37.5–1200 nM) of anti-(VEGF-D) mAbs for one hour at 25 °C in NaCl/P_i prior to injection over the sensor surface. For determination of the apparent binding affinities of mAbs for human VEGF-DΔNΔC, data were analysed using BIA evaluation 3.0 (BIAcore, Uppsala, Sweden) as described previously [37], using regions of the curves where 1 : 1 Langmuir binding was operative.

Epitope mapping. Multideterminant epitope mapping using the VEGF-D mAbs was performed as described previously [38] except that the primary antibodies were immobilized directly rather than using an entrapping antibody and that the use of parallel channels was possible using the BIAcore 2000. Anti-(VEGF-D) mAbs were coupled to individual channels of a CM5 sensor chip using amine coupling chemistry as described above. A target level of 3000 response units (RU) was set. The individual levels achieved were: VD1, 3179 RU; VD2, 3431 RU; VD3, 2834 RU; and VD4, 3092 RU. VEGF-DΔNΔC was then passed over the surfaces (30 µL, 105 µg·mL⁻¹) at a flow rate of 10 µL·min⁻¹. The free antibodies were passed over the captured antigen (30 µL, 40 µg·mL⁻¹) at the same flow rate. The surface was regenerated between cycles using 10 mM NaOH.

Human microvascular endothelial cell proliferation assay

Human microvascular endothelial cells (HMVECs) were grown in EBM containing 5% fetal bovine serum and growth supplements including epidermal growth factor and bovine brain extract as specified by the commercial supplier (Clonetics, Walkersville, MD, USA). For the assay, cells were removed with trypsin, washed and resuspended in complete medium, and aliquoted at 5×10^3 cells per well in a 24-well plate. Cells were allowed to adhere for 16 h at 37 °C after which they were incubated in EBM containing recombinant VEGF-DΔNΔC and 2% fetal bovine serum without epidermal growth factor and bovine brain extract. After 72 h of growth at 37 °C the cellular proliferation was quantified by cell counting.

RESULTS

Specificity and affinity of anti-(VEGF-D) mAbs

Four anti-(VEGF-D) mAbs, designated VD1, VD2, VD3 and VD4, all of the IgG₁ isotype, were raised in mice against human

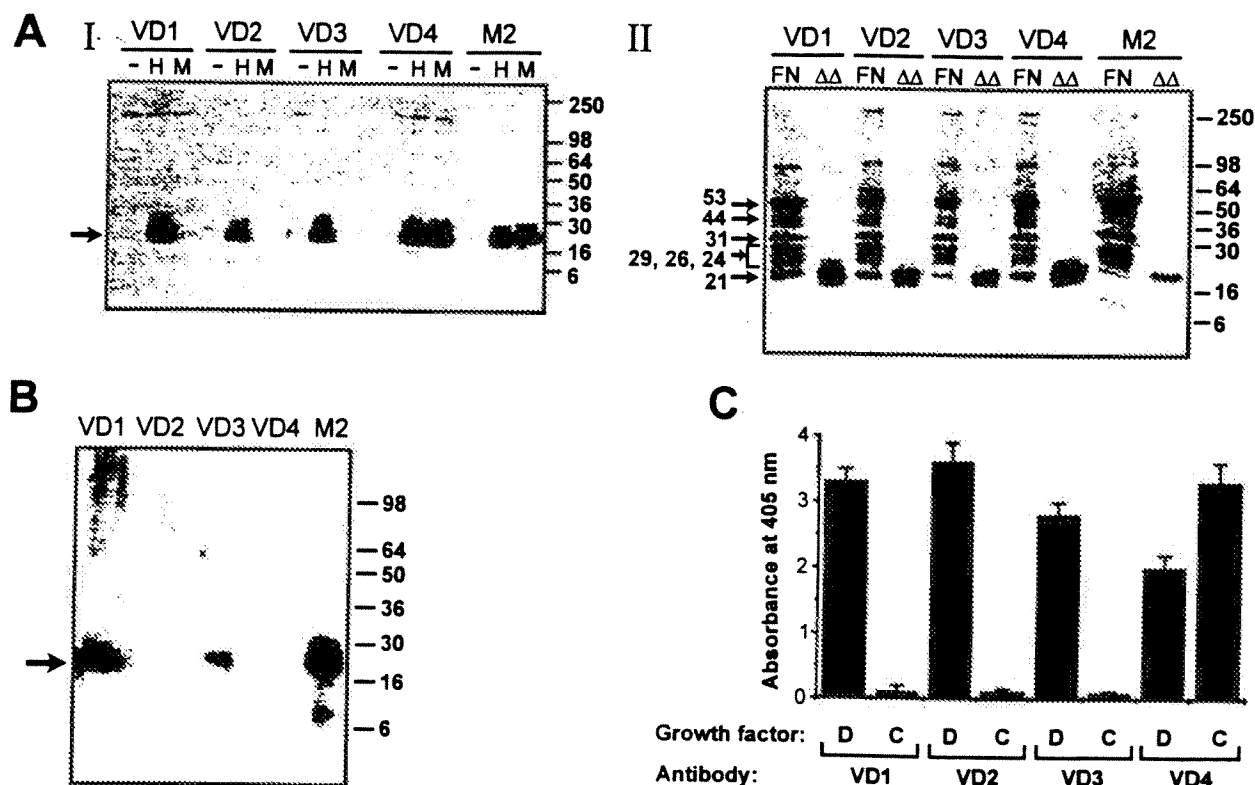


Fig. 1. Species cross-reactivity and specificity within the VEGF family of anti-(VEGF-D) mAbs. (A) Immunoprecipitation of human and mouse VEGF-D Δ N Δ C (I) and human full-length VEGF-D (II). I. Purified human (H) or mouse (M) VEGF-D Δ N Δ C were added to cell culture media and immunoprecipitated with M2 or anti-(VEGF-D) mAbs and protein A-Sepharose as described in Materials and methods. The mAb used for each immunoprecipitation is indicated at the top of the figure. Negative control immunoprecipitations (-) were from media to which recombinant protein had not been added. The products of immunoprecipitation were subjected to SDS/PAGE under reducing conditions and detected by western blot analysis with M2 (anti-FLAG) mAb. The black arrow denotes the positions of human or mouse VEGF-D Δ N Δ C (M_r 21 000) and numbers to the right denote the M_r of molecular mass markers (in K). II. Metabolically labeled polypeptides were immunoprecipitated with M2 or anti-(VEGF-D) mAbs (indicated at the top of the figure) from the conditioned media of cell lines expressing human VEGF-D-FULL-N-FLAG (FN) or human VEGF-D Δ N Δ C ($\Delta\Delta$). The cell line expressing VEGF-D-FULL-N-FLAG secretes full-length VEGF-D (M_r 53 000), partially processed forms (44 000, 31 000, 26 000 and 24 000), the N-terminal propeptide (10 000), the C-terminal propeptide (29 000) and the VHD (21 000) as detected previously with VEGFR-3-Ig [24]. Products of immunoprecipitation were subjected to SDS/PAGE under reducing conditions and detected with a phosphorimager. Black arrows denote the positions of the derivatives of VEGF-D-FULL-N-FLAG and of VEGF-D Δ N Δ C and the associated numbers indicate the M_r (in K) of these polypeptides. Numbers to the right denote the M_r of molecular mass markers (in K). (B) Western blot analysis with anti-(VEGF-D) mAbs. Purified human VEGF-D Δ N Δ C (1 μ g per track) was subjected to SDS/PAGE under reducing conditions and western blot analysis with M2 or anti-(VEGF-D) mAbs (indicated at the top of the figure). Filters were incubated with mAbs at a concentration of 50 μ g mL $^{-1}$. The black arrow denotes the position of human VEGF-D Δ N Δ C and numbers to the right denote the M_r of molecular mass markers (in K). (C) Analysis of the binding of mAbs to human VEGF-D Δ N Δ C and human VEGF-C Δ N Δ C by enzyme immunoassay. Microtitre plates were coated with growth factors to which purified mAbs were subsequently added. Plates were incubated, washed and developed as described in Materials and methods and the assays quantified by reading absorbance at 405 nm. The growth factors, human VEGF-D Δ N Δ C (D) or human VEGF-C Δ N Δ C (C), and the mAbs included in each incubation are indicated under the x-axis. Each column represents the mean absorbance from two assays and error bars denote the range of absorbance measured.

VEGF-D Δ N Δ C, a recombinant form of the VHD of human VEGF-D [22], as described in Materials and methods. All mAbs were able to immunoprecipitate human VEGF-D Δ N Δ C from cell culture medium, although only VD4 was able to immunoprecipitate mouse VEGF-D Δ N Δ C (Fig. 1A). *In vivo*, VEGF-D is initially synthesized as a precursor protein (full-length VEGF-D) containing N-terminal and C-terminal propeptides that are subsequently proteolytically cleaved from the VHD [24]. In order to determine if the mAbs were able to bind unprocessed VEGF-D (i.e. before removal of the N-terminal and C-terminal propeptides), mAbs were used to immunoprecipitate full-length VEGF-D by incubation with the conditioned culture medium of metabolically labeled cells stably transfected with an expression construct for VEGF-D-FULL-N-FLAG [24]. This cell line secretes full-length VEGF-D (M_r

53 000), numerous partially processed forms, both propeptides and the fully processed form consisting only of the VHD [24]. All four mAbs immunoprecipitated full-length VEGF-D from the medium of these cells, indicating that the N-terminal and C-terminal propeptides in the full-length form do not block the binding of the mAbs to the VHD (Fig. 1A). In addition, all mAbs immunoprecipitated the same partially processed forms and the fully processed form (M_r 21 000), indicating that the epitopes of the VHD recognized by the mAbs are accessible in the various intermediates produced during VEGF-D biosynthesis.

In western blot analysis, human VEGF-D Δ N Δ C was clearly detected with VD1 whereas it was barely detectable with VD3 and undetectable with VD2 and VD4 (Fig. 1B), indicating that the mAbs bind epitopes with varying susceptibility to

Table 1. Kinetic data derived from biosensor analysis of the interaction between immobilized anti-(VEGF-D) mAbs and VEGF-DΔNΔC.

Antibody	k_a ($1 \cdot M^{-1} \cdot s^{-1}$)	k_d ($1 \cdot s^{-1}$)	K_D (M)
VD1	7.4×10^4	2.2×10^{-3}	3.0×10^{-8}
VD2	1.1×10^5	3.9×10^{-3}	3.6×10^{-8}
VD3	8.6×10^4	5.2×10^{-3}	6.1×10^{-8}
VD4	7.8×10^4	4.5×10^{-3}	5.7×10^{-8}

denaturation. All four mAbs were tested in an enzyme immunoassay for cross-reactivity with VEGF-C, the most closely related protein to VEGF-D. All mAbs bound human VEGF-DΔNΔC in the immunoassay but only VD4 bound human VEGF-CΔNΔC (Fig. 1C), a recombinant form of the VHD of human VEGF-C [26]. Furthermore, mAbs VD1, VD2 and VD3 were unable to immunoprecipitate VEGF-CΔNΔC or recognize this ligand by western blot analysis (data not shown). These findings demonstrate that VD1, VD2 and VD3 are specific for VEGF-D. The observation that only VD4 binds mouse VEGF-DΔNΔC and human VEGF-CΔNΔC indicates that this mAb binds to a conserved region in the structures of VEGF-D and VEGF-C.

The relative affinities of the mAbs for human VEGF-DΔNΔC were determined by analysis of the binding kinetics for these interactions by biosensor studies using surface plasmon resonance detection [35]. Each of the mAbs was immobilized onto a sensor chip as described in Materials and methods (VD1, 4739 RU; VD2, 5268 RU; VD3, 5781 RU; and VD4, 5634 RU immobilized corresponding to 4.7, 5.2, 5.7 and 5.6 ng·mm⁻², respectively [39]) and binding curves were obtained by flowing human VEGF-DΔNΔC over the surface (41–689 nM) at a flow rate of 10 μL·min⁻¹. The binding constants (Table 1) were obtained by analysis of the initial dissociation phase to obtain the k_d , which was then used to constrain a global analysis of the association region of the curves, where a 1 : 1 Langmuir model was operative. As the antibodies were immobilized, a valency of 1 was assumed for the ligand. All antibodies displayed similar high affinity (K_D s of 30–61 nM) with apparent k_a s of between 7.4 and 11×10^4 M⁻¹·s⁻¹ and k_d s between 2.2 and 5.2×10^{-3} s⁻¹.

Table 2. Biosensor epitope mapping of anti-(VEGF-D) mAbs. Epitope mapping was performed as described in Materials and methods. The numbers denote binding levels (RU) obtained upon injection of mAb over a biosensor chip containing a complex consisting of VEGF-DΔNΔC bound to the immobilized mAb. Levels > 50 RU were taken as positive based on background levels observed when the experiment was performed in the absence of ligand.

Immobilized antibody	Injected antibody			
	VD1	VD2	VD3	VD4
VD1	21	4	4	247
VD2	26	–5	4	218
VD3	36	22	25	65
VD4	289	445	223	154

Epitope mapping

Multideterminant epitope mapping using the VEGF-D mAbs and the BIAcore 2000 biosensor was performed as described in Materials and methods. The use of amine coupling chemistry to couple mAbs to sensor chips did not interfere with VEGF-D binding as shown by the ability of all immobilized antibodies to bind ligand (VD1, 225 RU; VD2, 295 RU; VD3, 126 RU; VD4, 232 RU). The ability of mAbs in solution to bind VEGF-DΔNΔC-immobilized mAb complexes is shown in Table 2. Antibody VD4 was clearly able to bind when VEGF-DΔNΔC was in a complex with any of the other three immobilized mAbs. In contrast, VD1, VD2 and VD3 were unable to bind

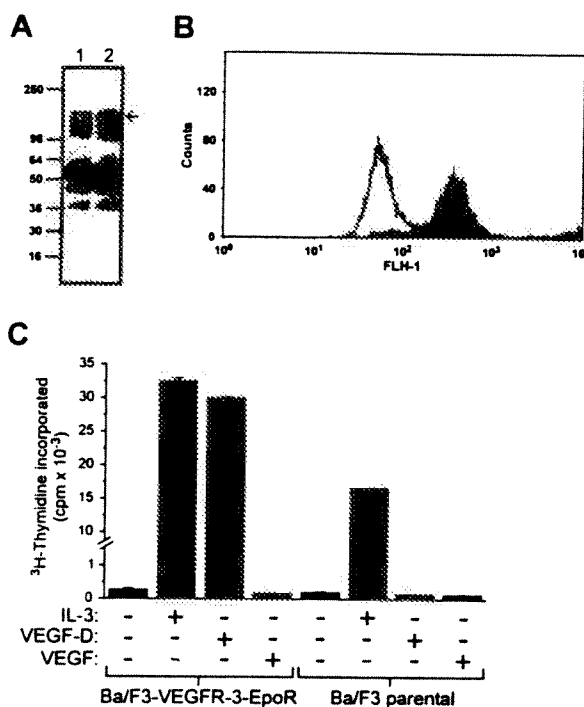
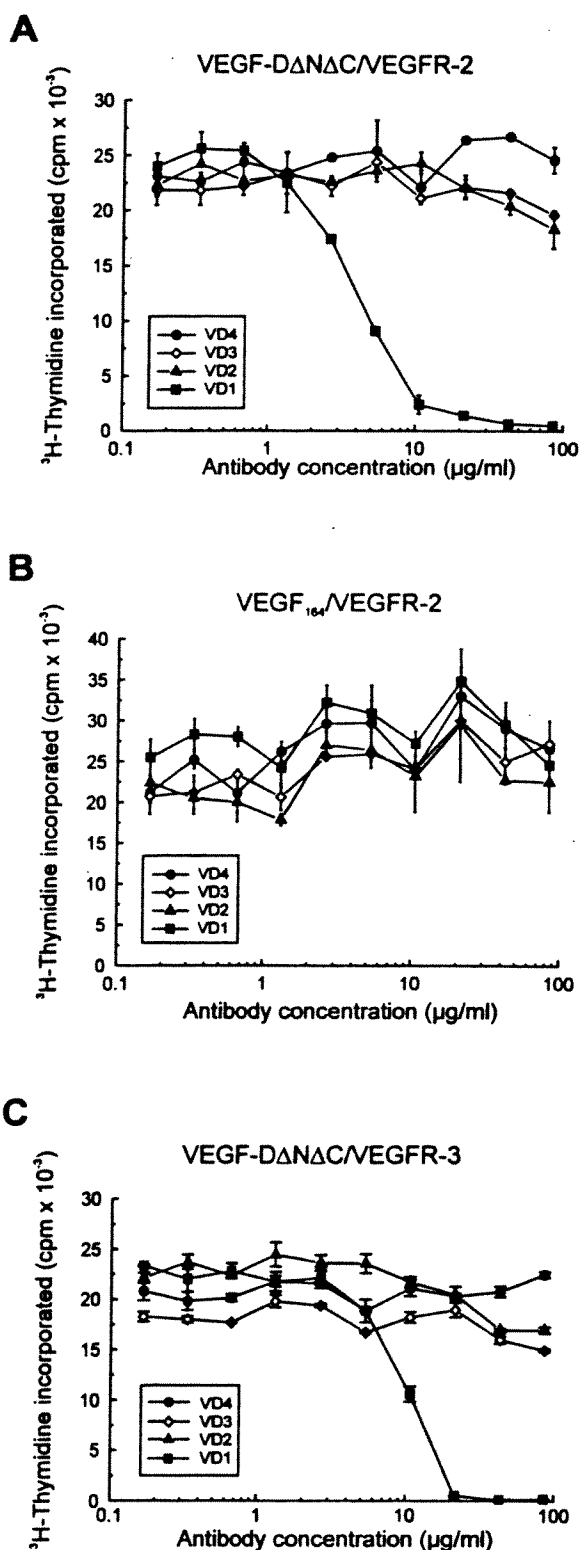


Fig. 2. Generation of the Ba/F3-VEGFR-3-EpoR cell line. (A) Ba/F3 cells expressing a chimeric receptor consisting of the extracellular domain of human VEGFR-3 and the transmembrane and cytoplasmic domains of mouse EpoR were identified by immunoprecipitation and western blot analysis using anti-VEGFR-3 polyclonal antibodies as described in Materials and methods. The sample in track 1 was derived from Ba/F3 cells that did not express the receptor whereas that in track 2 was from cells strongly expressing the receptor (Ba/F3-VEGFR-3-EpoR cells). The arrow to the right denotes the position of the chimeric receptor ($M_r \approx 150$ kDa) and numbers to the left denote the positions of molecular mass markers (in kDa). (B) Expression of the chimeric receptor was confirmed by flow cytometry. The Ba/F3-VEGFR-3-EpoR cells (shaded) and parental Ba/F3 cells (unshaded) were stained with anti-VEGFR-3 mAb. The small signal at high fluorescence ($> 5 \times 10^3$ on the FLH-1 scale) is due to aggregated cells. (C) The responses of the Ba/F3-VEGFR-3-EpoR and the parental Ba/F3 cell lines to IL-3, human VEGF-DΔNΔC (VEGF-D) and mouse VEGF₁₆₄ (VEGF) were monitored using the bioassay protocol described in Materials and methods. Cells were incubated in media containing IL-3 (100 ng·mL⁻¹), VEGF-DΔNΔC (500 ng·mL⁻¹) or VEGF₁₆₄ (100 ng·mL⁻¹) for 48 h at 37 °C. DNA synthesis was then quantified by the addition ³H-thymidine, incubation for 4 h, automated harvesting and β-counting. Values are expressed as mean ± SD.

VEGF- Δ N Δ C in complex with either immobilized VD1, VD2 or VD3. These results indicate that VD1, VD2 and VD3 recognize similar, or identical, epitopes whereas VD4 binds a distinct epitope. Interestingly, VD4 in solution was capable of further binding to VEGF- Δ N Δ C in complex with

immobilized VD4 (Table 2). The other mAbs did not exhibit further binding when ligand was bound to the same immobilized mAb. This demonstrates that only in the case of VD4 does VEGF- Δ N Δ C bind immobilized mAb in such an orientation that the second mAb-binding site of the dimeric ligand is inaccessible to the immobilized mAb. This further illustrates that the epitope recognized by VD4 is distinct from those recognized by the other three mAbs.



VEGF-D mAbs block activation of cell surface VEGFR-2 and VEGFR-3 chimeric receptors

As endothelial cells express several different VEGF receptors, which could potentially complicate the evaluation of the binding and activation of VEGF receptors by ligands, we established an assay that would only be responsive to signaling induced by dimerization of VEGFR-3. A chimeric molecule containing the extracellular domain of human VEGFR-3 and the transmembrane and cytoplasmic domains of the mouse EpoR was produced and stably expressed in the IL-3 dependent cell line Ba/F3 as described in Materials and methods. The chimeric molecule was used as members of the receptor-type tyrosine kinase family signal poorly in hematopoietic cells such as Ba/F3, whereas signaling from the EpoR cytoplasmic domain leads to cell survival and proliferation in the absence of IL-3 [40]. Cells expressing the chimeric receptor were initially selected by immunoprecipitation and western blot analysis with anti-(human VEGFR-3) antibodies (Fig. 2A) and receptor expression was subsequently confirmed by flow cytometry (Fig. 2B). The cell line expressing the chimeric receptor (designated Ba/F3-VEGFR-3-EpoR) can be rescued with VEGF- Δ N Δ C in the absence of IL-3 (Fig. 2C). In contrast, the parental cell line, which does not express VEGFR-2 or VEGFR-3, does not respond to VEGF- Δ N Δ C (Fig. 2C), indicating that the response of the Ba/F3-VEGFR-3-EpoR cell line to this ligand is totally dependent on the chimeric receptor. A Ba/F3 cell line expressing a chimeric receptor containing the extracellular domain of mouse VEGFR-2 and the transmembrane and cytoplasmic domains of EpoR (Ba/F3-VEGFR-2-EpoR cells) [22,27] was also used in this study. This cell line is responsive to VEGF- Δ N Δ C in the absence of IL-3 [22].

mAbs were tested for the capacity to block the activation of VEGFR-2 and VEGFR-3 in bioassays using Ba/F3-VEGFR-2-EpoR cells or Ba/F3-VEGFR-3-EpoR cells. Addition of antibodies that block the binding of VEGF- Δ N Δ C to the extracellular domains of the chimeric receptors or the subsequent cross-linking of the extracellular domains will cause cell death in the absence of IL-3, even in the presence of VEGF- Δ N Δ C. The effects of the anti-(VEGF-D) mAbs on the proliferative response of Ba/F3-VEGFR-2-EpoR cells to

Fig. 3. The effects of anti-(VEGF-D) mAbs on the responses of Ba/F3-VEGFR-2-EpoR cells to (A) VEGF- Δ N Δ C and (B) VEGF₁₆₄ and (C) of Ba/F3-VEGFR-3-EpoR cells to VEGF- Δ N Δ C. Samples of purified human VEGF- Δ N Δ C or mouse VEGF₁₆₄ were incubated with varying amounts of antibodies for one hour at 4 °C in NaCl/Pi before dilution of the mixtures 1 : 10 with IL-3-deficient cell culture medium. The resulting media contained approximately 500 ng·mL⁻¹ of VEGF- Δ N Δ C or 100 ng·mL⁻¹ of VEGF₁₆₄ and varying concentrations of mAbs as shown in the graphs. Cells were incubated in the media for 48 h at 37 °C and DNA synthesis was then quantified by ³H-thymidine incorporation. Each point on the graphs represents the mean c.p.m. incorporated from two assays and error bars denote the range of c.p.m. measured.

human VEGF-D Δ N Δ C are shown in Fig. 3A. VD1 blocked the response to VEGF-D Δ N Δ C in a dose-dependent fashion. Inclusion of VD1 at 10 $\mu\text{g}\cdot\text{mL}^{-1}$ in the cell culture medium (approximately a five-fold molar excess of mAb to VEGF-D Δ N Δ C) almost totally blocked the response of the cells. In contrast, mAbs VD2 and VD3, at a concentration of nearly 100 $\mu\text{g}\cdot\text{mL}^{-1}$ (approximately a 50-fold molar excess of mAb to VEGF-D Δ N Δ C), had partial inhibitory effects on the response, whereas VD4 had no detectable effect. As a control for specificity, mAbs were tested for the capacity to block the proliferative response of Ba/F3-VEGFR-2-EpoR cells to purified mouse VEGF₁₆₄, an alternative ligand for VEGFR-2 (Fig. 3B). None of the mAbs had any significant effect on the response of the cells to mouse VEGF₁₆₄ even at a 250-fold molar excess of mAb to the growth factor. The effects of the mAbs on the proliferative response of Ba/F3-VEGFR-3-EpoR cells to VEGF-D Δ N Δ C were similar to those observed for Ba/F3-VEGFR-2-EpoR cells (Fig. 3C) as the presence of mAb VD1 at 20 $\mu\text{g}\cdot\text{mL}^{-1}$ (a 10-fold molar excess to VEGF-D Δ N Δ C) totally blocked the response, much higher concentrations of VD2 and VD3 had only marginal effects and VD4 had no detectable effect.

Given that all four mAbs bind VEGF-D Δ N Δ C with similar high affinity (Table 2), the difference in the ability of the mAbs to inhibit the responses of the Ba/F3-VEGFR-3-EpoR and Ba/F3-VEGFR-2-EpoR cell lines to VEGF-D Δ N Δ C most likely reflects binding of mAbs to distinct epitopes. These results are therefore consistent with the conclusions drawn from the epitope mapping as they indicate that VD4 binds to a distinct epitope in comparison to the other three mAbs. The finding that VD2 and VD3 inhibited the response to both cell lines, but not as potently as VD1, suggests that the epitope to which VD1 binds is similarly located, but distinct, from the epitope(s) to which VD2 and VD3 bind.

VEGF-D mAbs block binding to immobilized VEGFR-2 and VEGFR-3

The inhibitory effects of anti-(VEGF-D) mAbs in the bioassays described above could be due to mAbs blocking the binding of ligand to receptor or by preventing receptor cross-linking. The bioassays cannot distinguish between inhibition by these two distinct mechanisms. In order to directly study the effect of the mAbs on the binding of VEGF-D Δ N Δ C to receptors, the interaction of this ligand with immobilized receptor extracellular domains was analysed with a biosensor. The extracellular domain of mouse VEGFR-2 (VEGFR-2-FLAG) and a chimeric protein consisting of the extracellular domain of human VEGFR-3 and the Fc portion of human IgG₁ (VEGFR-3-Ig) were immobilized onto sensor chips as described in Materials and methods (4677 and 5113 RU immobilized equivalent to 4.7 and 5.1 ng $\cdot\text{mm}^{-2}$, respectively). The effects of mAbs on receptor interactions were determined by flowing mixtures of human VEGF-D Δ N Δ C, preincubated with varying concentrations of mAbs, over the sensor chips at a flow rate of 10 $\mu\text{L}\cdot\text{min}^{-1}$ (Fig. 4). mAb VD1 strongly inhibited the binding of VEGF-D Δ N Δ C to both VEGFR-2 and VEGFR-3. Preincubation of human VEGF-D Δ N Δ C with a three-fold molar excess of VD1 (a concentration of mAb of approximately 25 $\mu\text{g}\cdot\text{mL}^{-1}$) almost totally blocked binding to both receptors. mAbs VD2 and VD3 also inhibited interactions with both receptors but at higher mAb concentrations than for VD1. An approximately 24-fold molar excess of VD2 and VD3 (mAb concentration of approximately 190 $\mu\text{g}\cdot\text{mL}^{-1}$) was required to almost totally block binding to both receptors. In

contrast, VD4 had only marginal effects. The findings that VD2 and VD3 block interactions with the immobilized receptors, but less potently than VD1, whereas VD4 is not neutralizing, are consistent with the epitope mapping and bioassay studies described above that indicate a similar location on VEGF-D Δ N Δ C for the VD1-binding, VD2-binding and VD3-binding epitopes, but a distinct location for the VD4-binding epitope. Although similarly located, the VD1-binding

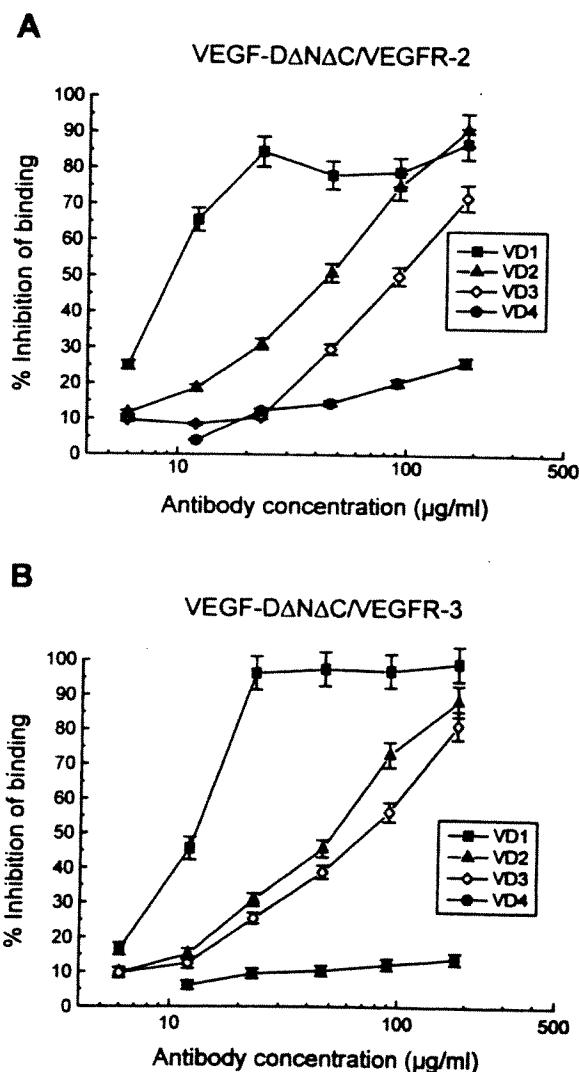


Fig. 4. Biosensor analysis of the effects of anti-(VEGF-D) mAbs on the binding of VEGF-D Δ N Δ C to immobilized (A) VEGFR-2 and (B) VEGFR-3 extracellular domains. VEGFR-2-FLAG and VEGFR-3-Ig were immobilized onto sensor chips as described in Materials and methods. After preincubation for 1 h at 25 °C, 30 μL aliquots of mixtures containing human VEGF-D Δ N Δ C at 2 $\mu\text{g}\cdot\text{mL}^{-1}$ and varying concentrations of mAbs as shown on the graphs were injected over the chip surfaces at a flow rate of 10 $\mu\text{L}\cdot\text{min}^{-1}$. The percentage inhibition of binding was calculated using the biosensor signals observed at the beginning of the dissociation phase in the presence of competitor (RU_c) and the signal observed with VEGF-D Δ N Δ C injected at 2 $\mu\text{g}\cdot\text{mL}^{-1}$ in the presence of a nonspecific control antibody (anti-epidermal growth factor receptor mAb 528 [52]) (RU_t) as follows: % Inhibition of binding = (RU_t - RU_c) \times 100/RU_t.

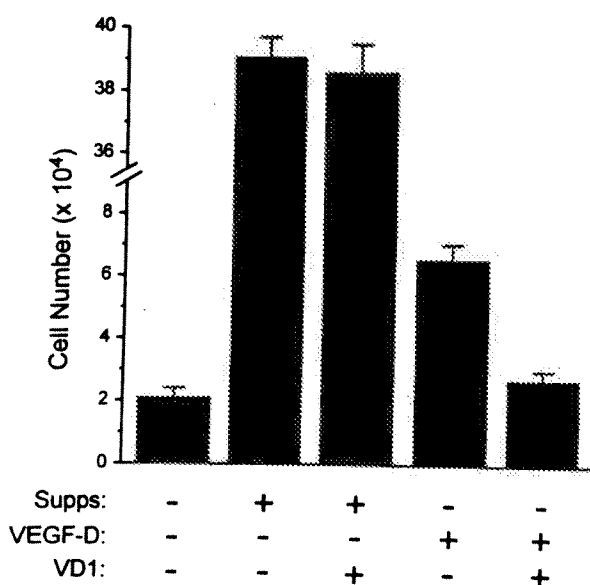


Fig. 5. Analysis of the capacity of mAb VD1 to block the activity of VEGF-D in an HMVEC proliferation assay. HMVEC cells (5×10^3) were incubated in medium supplemented with 500 ng mL^{-1} of human VEGF-D Δ N Δ C (VEGF-D) or with growth supplements not including VEGF-D (Supps), in the presence or absence of mAb VD1 ($185 \text{ } \mu\text{g mL}^{-1}$), for 72 h at 37 °C. After incubation, cellular growth was quantified by counting cells. Values are expressed as mean \pm SD.

epitope appears to be different from the VD2-binding and VD3-binding epitope(s).

Data from analyses of the effects of mAbs VD1 and VD4 on the interactions of VEGF-D Δ N Δ C with receptors in the Ba/F3 bioassays and the biosensor studies were concordant in that they demonstrated that VD1 blocks the interactions with VEGFR-2 and VEGFR-3 whereas VD4 does not. In contrast, the conclusions for VD2 and VD3 differ between the two systems as these mAbs had only weak effects in the bioassays but, at lower molar ratios of mAb to growth factor, clearly blocked the interactions of VEGF-D Δ N Δ C with both receptors in the biosensor study. This apparent discrepancy could be explained by different sensitivities of the two assay systems to free growth factor. Alternatively, the explanation could be that dissociation of the mAb-growth factor complex occurs to different degrees in the two systems. In the biosensor study, analysis of ligand-receptor interactions, after preincubation of mAb with growth factor, takes only a few minutes. Therefore the degree of dissociation of the mAb-growth factor complex prior to and during analysis may be limited. In the bioassay system, the mAb-growth factor complex is incubated with cells in culture medium for 48 h before thymidine incorporation is measured. Therefore the degree of dissociation of the mAb-growth factor complex may be greater. As a consequence, higher molar ratios of mAb to growth factor may be required to block ligand-receptor interactions in the bioassays than in the biosensor analysis.

mAb VD1 blocks the mitogenic response of microvascular endothelial cells to VEGF-D

An HMVEC proliferation assay was used to determine if mAb VD1 could block the mitogenic response of vascular

endothelial cells to VEGF-D. Previous studies demonstrated that the mitogenic response of vascular endothelial cells to VEGF is mediated via VEGFR-2, not VEGFR-1 [41], suggesting that the response to VEGF-D is most likely via VEGFR-2, although signaling via VEGFR-3 cannot be excluded. VEGF-D Δ N Δ C was clearly able to induce proliferation of HMVECs over a period of 72 h (Fig. 5). However, inclusion of mAb VD1 at a 40-fold molar excess to VEGF-D Δ N Δ C completely blocked this mitogenic response. In contrast, VD1 had no significant effect on the growth of cells stimulated with medium containing growth supplements (see Materials and methods) that did not include VEGF-D.

DISCUSSION

To explore the interactions between VEGF-D and its receptors, VEGFR-2 and VEGFR-3, VEGF-D mAbs were specifically raised to the mature form of VEGF-D, which consists of noncovalent homodimers of the VHD [24]. This approach was chosen to maximize the probability that the mAbs would block the interaction of VEGF-D with VEGFR-2 and VEGFR-3. Indeed, three of the mAbs, VD1, VD2 and VD3, block the binding to both receptors, although VD1 does so more potently. Furthermore, mAbs targeted to the VHD will be useful for immunohistochemical detection of bioactive VEGF-D, whereas mAbs raised to the propeptides would not be appropriate because, after cleavage from the VHD, the free propeptides must localize differently to the VHD in tissue as they are unable to bind VEGFR-2 and VEGFR-3.

In order to evaluate the neutralizing effects of the VEGF-D mAbs in an assay system that would be responsive to the binding and cross-linking of VEGFR-3 only, we avoided the use of *in vitro* cell lines or primary cultures of lymphatic endothelial cells that may express other VEGF receptors, in particular VEGFR-2. This excludes the possibility that other receptors could initiate signaling alone or as part of a heterodimeric complex with VEGFR-3. Instead, we developed a factor-dependent Ba/F3 cell line expressing a chimeric VEGFR-3/EpoR receptor. The approach of using a chimeric receptor tyrosine kinase/cytokine receptor was initially described by others [40] as a means of detecting the cross-linking of the ligand-binding domains of orphan receptors. The system works effectively for other receptors that rely on dimerization for signal transduction, for example VEGFR-2 [22,27] and epidermal growth factor receptor [40]. The VEGFR-3 bioassay cell line described here will be useful for further development of VEGFR-3 agonists and antagonists.

The biosensor analysis of the capacity of VEGF-D mAbs to block binding of mature VEGF-D to immobilized VEGFR-2 and VEGFR-3 revealed that the neutralizing mAbs, VD1, VD2 and VD3, each block the interaction to both receptors with similar potency. This finding indicates that VEGFR-2 and VEGFR-3 bind to very similar regions of mature VEGF-D. This is not surprising given that the extracellular ligand-binding domains of these two receptors are closely related in structure; they exhibit approximately 35% amino acid identity and contain seven immunoglobulin-like domains [19]. Moreover, the regions of VEGF involved in binding to VEGFR-1 and VEGFR-2 are in similar locations. All seven of the residues in VEGF, of moderate or great importance for binding to VEGFR-2, are either in, or just outside, the region that forms the interface with VEGFR-1 in the crystal structure of the VEGF-VEGFR-1 complex [42]. Therefore, the regions in the

VHDs of mammalian VEGF family members responsible for interactions with the VEGF receptors are likely to be clustered together. It is tempting to speculate that changes in the amino acid sequence of the VEGF epitope responsible for binding to VEGFR-1 generated the VEGFR-3 binding epitope in VEGF-D. However, this could only be determined from a crystal structure of the VEGF-D-VEGFR-3 complex. This structure has not yet been documented, nor has the structure of VEGF-D or the closely related VEGF-C. The finding that many of the amino acid residues required for VEGFR-1 binding by VEGF are conserved in a viral VEGF [43], which binds VEGFR-2 but not VEGFR-1, indicates that VEGF receptor binding epitopes are not easily predicted from the homology of the primary structures of VEGF family members.

VEGFR-2 is an important signaling molecule for the regulation of both embryonic and tumour development [11–13]. The known mammalian ligands for VEGFR-2, namely VEGF, VEGF-C and VEGF-D, are all expressed in numerous tissues during embryogenesis [25,44,45] and are localized in tumors ([46,47]; M. G. Achen, R. A. Williams, M. P. Mineleus, G. E. Thornton, K. Stevens, P. A. W. Rogers, F. Cederman, S. Roufail and S. A. Stacker, unpublished observations). VEGF is essential for vascularization of the embryo [2,3] and for angiogenesis in some tumours [4], although it is not expressed in all tumours [48,49]. In contrast, the importance of VEGF-D for developmental angiogenesis is unknown. VEGF-D may indeed play a role in tumour angiogenesis as it is angiogenic [23] and is expressed in human tumours (M. G. Achen, R. A. Williams, M. P. Mineleus, G. E. Thornton, K. Stevens, P. A. W. Rogers, F. Cederman, S. Roufail and S. A. Stacker, unpublished observations). Ultimately, specific inhibitors for each of the VEGF family members will be required to delineate their contributions to tumour angiogenesis. Therefore, the antibodies described here, in particular VDI, a mAb that blocks the interaction between VEGF-D and VEGFR-2 but does not bind VEGF-C, will be useful for studying the contribution of VEGF-D to tumour angiogenesis mediated by VEGFR-2. Furthermore, these mAbs will be useful for analysis of the role of VEGF-D in other conditions characterized by excess or inappropriate angiogenesis such as rheumatoid arthritis, cirrhosis of the liver, chronic periodontitis, idiopathic pulmonary fibrosis, psoriasis, proliferative retinopathies and age-related macular degeneration.

As VEGF-D activates VEGFR-3 [22], a receptor that is expressed on lymphatic endothelial cells in adult tissues [32] and is thought to signal for lymphangiogenesis [19], VEGF-D expressed in solid tumours may induce lymphangiogenesis as well as angiogenesis. It is well known that some tumours metastasize via blood vessels and others via the lymphatic vessels. It may be that the route of metastatic spread of a tumour is influenced by its capacity to induce angiogenesis or lymphangiogenesis. Therefore, expression by a tumour of a growth factor such as VEGF, which is angiogenic but not lymphangiogenic [17], may favour spread via blood vessels whereas expression of VEGF-D, which can activate VEGFR-3 on the lymphatic endothelium, may favour spread by lymphatic vessels. The mAbs described here, which block the binding of VEGF-D, but not VEGF-C, to VEGFR-3, will be useful for analysing lymphangiogenesis induced by VEGF-D and its contribution to metastatic spread. In addition the mAbs could be used to investigate the role of VEGF-D in diseases primarily characterized by proliferation of lymphatic endothelial cells such as lymphangiomias [50] and Kaposi's sarcoma [51].

ACKNOWLEDGEMENTS

We are grateful to the Anti-Cancer Council of Victoria and the National Health and Medical Research Council of Australia for financial support, to Andrew Nash for provision of HMVECs and to Tony Burgess for critical reading of the manuscript.

REFERENCES

1. Achen, M.G. & Stacker, S.A. (1998) The vascular endothelial growth factor family: proteins which guide the development of the vasculature. *Int. J. Exp. Path.* **79**, 255–265.
2. Carmeliet, P., Ferreira, V., Breier, G., Pollofeyt, S., Keickens, L., Gertenstein, M., Fahrig, M., Vandenhoek, A., Harpal, K., Eberhardt, C., Declercq, C., Pawling, J., Moons, L., Collen, D., Risau, W. & Nagy, A. (1996) Abnormal blood vessel development and lethality in embryos lacking a single VEGF allele. *Nature* **380**, 435–439.
3. Ferrara, N., Carver-Moore, K., Chen, H., Dowd, M., Lu, L., O'Shea, K.S., Powell-Braxton, L., Hillan, K.J. & Moore, M.W. (1996) Heterozygous embryonic lethality induced by targeted inactivation of the VEGF gene. *Nature* **380**, 439–443.
4. Kim, K.J., Li, B., Winer, J., Armanini, M., Gillett, N., Phillips, H.S. & Ferrara, N. (1993) Inhibition of vascular endothelial growth factor-induced angiogenesis suppresses tumour growth *in vivo*. *Nature* **362**, 841–844.
5. Saleh, M., Stacker, S.A. & Wilks, A.F. (1996) Inhibition of growth of C6 glioma cells *in vivo* by expression of antisense vascular endothelial growth factor sequence. *Cancer Res.* **56**, 393–401.
6. De Vries, C., Escobedo, J.A., Ueno, H., Houck, K., Ferrara, N. & Williams, L.T. (1992) The fms-like tyrosine kinase, a receptor for vascular endothelial growth factor. *Science* **255**, 989–991.
7. Peters, K.G., De Vries, C. & Williams, L.T. (1993) Vascular endothelial growth factor receptor expression during embryogenesis and tissue repair suggests a role in endothelial differentiation and blood vessel growth. *Proc. Natl Acad. Sci. USA* **90**, 8915–8919.
8. Millauer, B., Witzmann-Voos, S., Schnürch, H., Martinez, R., Moller, N.P.H., Risau, W. & Ullrich, A. (1993) High affinity VEGF binding and developmental expression suggest Flk-1 as a major regulator of vasculogenesis and angiogenesis. *Cell* **72**, 835–846.
9. Quinn, T.P., Peters, K.G., De Vries, C., Ferrara, N. & Williams, L.T. (1993) Fetal liver kinase 1 is a receptor for vascular endothelial growth factor and is selectively expressed in vascular endothelium. *Proc. Natl Acad. Sci. USA* **90**, 7533–7537.
10. Plate, K.H., Breier, G., Millauer, B., Ullrich, A. & Risau, W. (1993) Up-regulation of vascular endothelial growth factor and its cognate receptors in a rat glioma model of tumor angiogenesis. *Cancer Res.* **53**, 5822–5827.
11. Shalaby, F., Rossant, J., Yamaguchi, T.P., Gertsenstein, M., Wu, X.F., Breitman, M.L. & Schuh, A.C. (1995) Failure of blood-island formation and vasculogenesis in flk-1-deficient mice. *Nature* **376**, 62–66.
12. Millauer, B., Shawver, L.K., Plate, K.H., Risau, W. & Ullrich, A. (1994) Glioblastoma growth inhibited *in vivo* by a dominant negative Flk-1 mutant. *Nature* **367**, 576–579.
13. Millauer, B., Longhi, M.P., Plate, K.H., Shawver, L.K., Risau, W., Ullrich, A. & Strawn, L.M. (1996) Dominant-negative inhibition of Flk-1 suppresses the growth of many tumor types *in vivo*. *Cancer Res.* **56**, 1615–1620.
14. Joukov, V., Pajusola, K., Kaipainen, A., Chilov, D., Lahtinen, I., Kukk, E., Saksela, O., Kalkkinen, N. & Alitalo, K. (1996) A novel vascular endothelial growth factor, VEGF-C, is a ligand for the Flt-4 (VEGFR-3) and KDR (VEGFR-2) receptor tyrosine kinases. *EMBO J.* **15**, 290–298.
15. Witzmannbichler, B., Asahara, T., Murohara, T., Silver, M., Spyridopoulos, I., Magner, M., Principe, N., Kearney, M., Hu, J.-S. & Isner, J.M. (1998) Vascular endothelial growth factor-C (VEGF-C/VEGF-2) promotes angiogenesis in the setting of tissue ischemia. *Am. J. Pathol.* **153**, 381–394.
16. Cao, Y., Linden, P., Farnebo, J., Cao, R., Eriksson, A., Kumar, V., Qi,

- J.H., Claesson-Welsh, L. & Alitalo, K. (1998) Vascular endothelial growth factor C induces angiogenesis *in vivo*. *Proc. Natl Acad. Sci. USA* 95, 14389–14394.
17. Oh, S.-J., Jeltsch, M.M., Birkenhäger, R., McCarthy, J.E.G., Weich, H.A., Christ, B., Alitalo, K. & Wiltling, J. (1997) VEGF and VEGF-C: specific induction of angiogenesis and lymphangiogenesis in the differentiated avian chorioallantoic membrane. *Dev. Biol.* 188, 96–109.
18. Jeltsch, M., Kaipainen, A., Joukov, V., Meng, X., Lakso, M., Rauvala, H., Swartz, M., Fukumura, D., Jain, R.K. & Alitalo, K. (1997) Hyperplasia of lymphatic vessels in VEGF-C transgenic mice. *Science* 276, 1423–1425.
19. Taipale, J., Mäkinen, T., Arighi, E., Kukk, E., Karkkainen, M. & Alitalo, K. (1999) Vascular endothelial growth factor receptor-3. *Curr. Top. Microbiol. Immunol.* 237, 85–96.
20. Kaipainen, A., Korhonen, J., Mustonen, T., van Hinsbergh, V.W., Fang, G.H., Dumont, D., Breitman, M. & Alitalo, K. (1995) Expression of the *fms*-like tyrosine kinase 4 gene becomes restricted to lymphatic endothelium during development. *Proc. Natl Acad. Sci. USA* 92, 3566–3570.
21. Orlandini, M., Marconcini, L., Ferruzzi, R. & Oliviero, S. (1996) Identification of a *c-fos*-induced gene that is related to the platelet-derived growth factor/vascular endothelial growth factor family. *Proc. Natl Acad. Sci. USA* 93, 11675–11680.
22. Achen, M.G., Jeltsch, M., Kukk, E., Mäkinen, T., Vitali, A., Wilks, A.F., Alitalo, K. & Stacker, S.A. (1998) Vascular endothelial growth factor D (VEGF-D) is a ligand for the tyrosine kinases VEGF receptor 2 (Flk-1) and VEGF receptor 3 (Flt-4). *Proc. Natl Acad. Sci. USA* 95, 548–553.
23. Marconcini, L., Marchio, S., Morbidelli, L., Cartocci, E., Albini, A., Ziche, M., Bussolino, F. & Oliviero, S. (1999) *c-fos*-induced growth factor/vascular endothelial growth factor D induces angiogenesis *in vivo* and *in vitro*. *Proc. Natl Acad. Sci. USA* 96, 9671–9676.
24. Stacker, S.A., Stenvers, K., Caesar, C., Vitali, A., Domagala, T., Nice, E., Roufail, S., Simpson, R.J., Moritz, R., Karpanen, T., Alitalo, K. & Achen, M.G. (1999) Biosynthesis of vascular endothelial growth factor-D involves proteolytic processing which generates non-covalent homodimers. *J. Biol. Chem.* 274, 32127–32136.
25. Avantiagato, V., Orlandini, M., Acampora, D., Oliviero, S. & Simeone, A. (1998) Embryonic expression pattern of the murine *figf* gene, a growth factor belonging to platelet-derived growth factor/vascular endothelial growth factor family. *Mech. Dev.* 73, 221–224.
26. Joukov, V., Sorsa, T., Kumar, V., Jeltsch, M., Claesson-Welsh, L., Cao, Y., Saksela, O., Kalkkainen, N. & Alitalo, K. (1997) Proteolytic processing regulates receptor specificity and activity of VEGF-C. *EMBO J.* 16, 3898–3911.
27. Stacker, S.A., Vitali, A., Caesar, C., Domagala, T., Groenen, L.C., Nice, E., Achen, M.G. & Wilks, A.F. (1999) A mutant form of vascular endothelial growth factor (VEGF) that lacks VEGF receptor-2 activation retains the ability to induce vascular permeability. *J. Biol. Chem.* 274, 34884–34892.
28. Pajusola, K., Aprelikova, O., Korhonen, J., Kaipainen, A., Pertovaara, L., Alitalo, R. & Alitalo, K. (1992) FLT4 receptor tyrosine kinase contains seven immunoglobulin-like loops and is expressed in multiple human tissues and cell lines. *Cancer Res.* 52, 5738–5743.
29. D'Andrea, A.D., Lodish, H.F. & Wong, G.G. (1989) Expression cloning of the murine erythropoietin receptor. *Cell* 57, 277–285.
30. Mizushima, S. & Nagata, S. (1990) pEF-BOS, a powerful mammalian expression vector. *Nucleic Acids Res.* 18, 5322.
31. Tybulewicz, V.L., Crawford, C.E., Jackson, P.K., Bronson, R.T. & Mulligan, R.C. (1991) Neonatal lethality and lymphopenia in mice with a homozygous disruption of the *c-abl* proto-oncogene. *Cell* 65, 1153–1163.
32. Lymboussaki, A., Partanen, T.A., Olofsson, B., Thomas-Crusells, J., Fletcher, C.D.M., de Waal, R.M.W., Kaipainen, A. & Alitalo, K. (1998) Expression of the vascular endothelial growth factor C receptor VEGFR-3 in lymphatic endothelium of the skin and in vascular tumors. *Am. J. Pathol.* 153, 395–403.
33. Bernardi, P., Patel, V.P. & Lodish, H.F. (1987) Lymphoid precursor cells adhere to two different sites on fibronectin. *J. Cell. Biol.* 105, 489–498.
34. Laemmli, U.K. (1970) Cleavage of structural proteins during the assembly of the head of bacteriophage T4. *Nature* 227, 680–685.
35. Nice, E.C. & Catimel, B. (1999) Instrumental biosensors: new perspectives for the analysis of biomolecular interactions. *Bioessays* 21, 339–352.
36. Catimel, B., Domagala, T., Nerrie, M., Weinstock, J., White, S., Abud, H., Heath, J. & Nice, E. (1999) Recent applications of instrumental biosensors for protein and peptide structure-function studies. *Protein Peptide Lett.* 6, 319–340.
37. Catimel, B., Nerrie, M., Lee, F.T., Scott, A.M., Ritter, G., Welt, S., Old, L.J., Burgess, A.W. & Nice, E.C. (1997) Kinetic analysis of the interaction between the monoclonal antibody A33 and its colonic epithelial antigen by the use of an optical biosensor. A comparison of immobilisation strategies. *J. Chromatogr. A* 776, 15–30.
38. Nice, E., Layton, J., Fabri, L., Hellman, U., Engstrom, A., Persson, B. & Burgess, A.W. (1993) Mapping of the antibody- and receptor-binding domains of granulocyte colony-stimulating factor using an optical biosensor. Comparison with enzyme-linked immunosorbent assay competition studies. *J. Chromatogr.* 646, 159–168.
39. Stenberg, E., Persson, B., Roos, H. & Urbaniczki, J. (1990) Quantitative determination of surface concentration of protein with surface plasmon resonance using radiolabeled proteins. *J. Colloid Interface* 43, 513–526.
40. Pacifici, R.E. & Thomason, A.R. (1994) Hybrid tyrosine kinase/cytokine receptors transmit mitogenic signals in response to ligand. *J. Biol. Chem.* 269, 1571–1574.
41. Keyt, B.A., Nguyen, H.V., Berleau, L.T., Duarte, C.M., Park, J., Chen, H. & Ferrara, N. (1996) Identification of vascular endothelial growth factor determinants for binding KDR and FLT-1 receptors. *J. Biol. Chem.* 271, 5638–5646.
42. Wiesmann, C., Fuh, G., Christinger, H.W., Eigenbrot, C., Wells, J.A. & de Vos, A.M. (1997) Crystal structure at 1.7 Å resolution of VEGF in complex with domain 2 of the Flt-1 receptor. *Cell* 91, 695–704.
43. Wise, L.M., Veikkola, T., Mercer, A.A., Savory, L.J., Fleming, S.B., Caesar, C., Vitali, A., Mäkinen, T., Alitalo, K. & Stacker, S.A. (1999) Vascular endothelial growth factor (VEGF)-like protein from orf virus NZ2 binds to VEGFR2 and neuropilin-1. *Proc. Natl Acad. Sci. USA* 96, 3071–3076.
44. Breier, G., Albrecht, U., Sterrer, S. & Risau, W. (1992) Expression of vascular endothelial growth factor during embryonic angiogenesis and endothelial cell differentiation. *Development* 114, 521–532.
45. Kukk, E., Lymboussaki, A., Taira, S., Kaipainen, A., Jeltsch, M., Joukov, V. & Alitalo, K. (1996) VEGF-C receptor binding and pattern of expression with VEGFR-3 suggests a role in lymphatic vascular development. *Development* 122, 3829–3837.
46. Salven, P., Heikkilä, P. & Joensuu, H. (1997) Enhanced expression of vascular endothelial growth factor in metastatic melanoma. *Br. J. Cancer* 76, 930–934.
47. Valtola, R., Salven, P., Heikkilä, P., Taipale, J., Joensuu, H., Rehn, M., Pihlajaniemi, T., Weich, H., de Waal, R. & Alitalo, K. (1999) VEGFR-3 and its ligand VEGF-C are associated with angiogenesis in breast cancer. *Am. J. Pathol.* 154, 1381–1390.
48. Kumar-Singh, S., Weyler, J., Martin, M.J., Vermeulen, P.B. & Van Marck, E. (1999) Angiogenic cytokines in mesothelioma: a study of VEGF, FGF-1 and -2, and TGF- β expression. *J. Pathol.* 189, 72–78.
49. Bayer-Garner, I.B., Hough, A.J.J. & Smoller, B.R. (1999) Vascular endothelial growth factor expression in malignant melanoma: prognostic versus diagnostic usefulness. *Mod. Pathol.* 12, 770–774.
50. Breiteneder-Geleff, S., Soleiman, A., Kowalski, H., Horvat, R., Amann, G., Kriehuber, E., Diem, K., Weninger, W., Tschachler, E., Alitalo, K. & Kerjaschki, D. (1999) Angiosarcomas express mixed endothelial phenotypes of blood and lymphatic capillaries. Podoplanin as a specific marker for lymphatic endothelium. *Am. J. Pathol.* 154, 385–394.

- artane . S v .
 Kunas W. d M A. re neder M. a C.
 We l K. i ne T. B te -Gele M e
 51. Val . . P t hl P E el J. tu ff. K r aschke D
 li o . H M schac or amm(999) S Ezi, i e v
 An heba gro h f or re e. - d pre pan of ts l a
 e do ha omie i acbl c pto 3 an podo l in ugge
 ly p/ uc end l al l origin of Kaposi's sarcoma tumor ells.
Lab. nves. 79, 243-251.

(Eur. J. Biochem. 267) 2515

- 5
 2. Kawamoto. T., Sato, J.D., Le, A., Polikoff, J., Sato, G.H. & Mendelsohn, J. (1983) Growth stimulation of A431 cells by epidermal growth factor: identification of high-affinity receptors for epidermal growth factor by an anti-receptor monoclonal antibody. *Proc. Natl Acad. Sci. USA* 80, 1337-1341.